Horizon 2020
Programme

GENIORS

Research and Innovation Action (RIA)

This project has received funding from the European Union's Horizon 2020 research and innovation programme under grant agreement No 755171.

Start date : 2017-06-01 Duration : 48 Months
http://geniors.eu/

GENIORS

Report on efficiencyof the electrochemical decomposition of ligands from SX processes and on its inputs on MABB precursor properties

Authors : Dr. Robin TAYLOR (NNL), C Maher (NNL), R Sanderson (NNL), H Colledge (NNL), J Holt (NNL), R Taylor (NNL)

GENIORS - Contract Number: 755171

Project officer: Roger Garbil

Document title	Report on efficiencyof the electrochemical decomposition of ligands from SX processes and on its inputs on MABB precursor properties
Author(s)	Dr. Robin TAYLOR, C Maher (NNL), R Sanderson (NNL), H Colledge (NNL), J Holt (NNL), R Taylor (NNL)
Number of pages	80
Document type	Deliverable
Work Package	WP7
Document number	D7.2
Issued by	NNL
Date of completion	2021-06-18 11:35:51
Dissemination level	Public

Summary

This report describes process steps needed at the interface between the separation and conversion (or finishing) processes. Specifically how to deal with the aqueous phase ligands that are carried over from the separation process which could adversely affect the quality of the mixed oxide products produced in the product finishing process (and hence MABB or homogeneous fuel fabrication). It outlines strategies including high temperature nitric acid and electrochemical decomposition and experiments that are designed to not only underpin these process steps but also to support their placement within the finishing flowsheet. Additional experiments focused on determining the effects of the ligands used in the i-SANEX and EURO-GANEX processes on the oxalate co-precipitation stage are described. The results indicate that these ligands have very limited effects on the oxalate precipitation stage and the favoured strategy of decomposing the ligands (in an evaporator and/or electrochemical process) in the lower activity oxalate mother liquor prior to recycling the nitric acid back into the process is credible.

Approval

Date	By
2021-07-01 08:42:07	Dr. Gilles LETURCQ (CEA)
2021-07-13 17:01:37	Dr. Jean-Marc ADNET (CEA)
2021-07-13 17:40:07	Mr. Stéphane BOURG (CEA)

CONTENT

This project has received funding from the EURATOM research and training programme 2014-2018 under grant agreement No 755171. The content of this deliverable reflects only the author's view. The European Commission is not responsible for any use that may be made of the information it contains.

This project has received funding from the EURATOM research and training programme 2014-2018 under grant agreement No 755171. The content of this deliverable reflects only the author's view. The European Commission is not responsible for any use that may be made of the information it contains.

LIST OF FIGURES

This project has received funding from the EURATOM research and training programme 2014-2018 under grant agreement No 755171. The content of this deliverable reflects only the author's view. The European Commission is not responsible for any use that may be made of the information it contains.

This project has received funding from the EURATOM research and training programme 2014-2018 under grant agreement No 755171. The content of this deliverable reflects only the author's view. The European Commission is not responsible for any use that may be made of the information it contains.

This project has received funding from the EURATOM research and training programme 2014-2018 under grant agreement No 755171. The content of this deliverable reflects only the author's view. The European Commission is not responsible for any use that may be made of the information it contains.

LIST OF TABLES

This project has received funding from the EURATOM research and training programme 2014-2018 under grant agreement No 755171. The content of this deliverable reflects only the author's view. The European Commission is not responsible for any use that may be made of the information it contains.

ABBREVIATION

AA	Acetic acid
AMSEL	SELective AMericium extraction
ADU	Ammonium DiUranate
AHA	AcetoHydroxamic Acid
CEA	French Alternative Energies and Atomic Energy Commission
CHALMEX	CHALmers GANEX process
CML	Concentrated Mother Liquor
COEX	CO-EXtraction
CV	Cyclic Voltametry
EXAm	AMercium EXtraction
DEO	Direct Electrochemical Oxidation
GANEX	Group ActNide EXtraction
ICP-MS	Inductive Coupled Plasma Mass Spectrometry
ICP-OES	Inductive Coupled Plasma Optical Emission Spectrometry
Nb/BDD	Niobium coated with Boron Doped Diamond
NEA	Nuclear Energy Authority
NHE	Normal Hydrogen Electrode
NNL	UK National Nuclear Laboratory
MA	Minor actinide
MDD	Mixed DeNitration
MEO	Mediated Electrochemical Oxidation
MEO(Ag)	Silver Mediated Electrochemical Oxidation
OML	Oxalate Mother Liquor
RDE	Rotating Disc Electrode
s-BTP	2-6-bis5-6-disulphophenyl-1-2-4-triazin-3-ylpyridine
Ti/Pt	Platinised titanium
PSU	Power Supply Unit
PTD	2,6-bis[1-(propan-1-ol)-1,2,3-triazol-4-yl)]pyridine
PUREX	Plutonium Uranium EXtraction
PVDF	PolyVinyliDene Fluoride
SANEX	Selective ActiNide EXtraction
SNF	Spent nuclear fuel
TDN	Thermal DeNitration
TPAEN	N,N,N′,N′-tetrakis[(6-carboxypyridin-2-yl)methyl]ethylenediamine
TRU	TRnsUranium
UV-Vis	UltraViolet VISible spectrometry
WAR	Weak Acid Resin

This project has received funding from the EURATOM research and training programme 2014-2018 under grant agreement No 755171. The content of this deliverable reflects only the author's view. The European Commission is not responsible for any use that may be made of the information it contains.

INTRODUCTION

The future recycling of spent nuclear fuels (SNF) using hydrometallurgical (solvent extraction based) processes will lead to various actinide nitrate products, depending on fuel cycle requirements at that time [1]. The trend is towards mixed actinide products that add further barriers to proliferation of nuclear materials (reduced 'attractiveness' of the products) and simplify downstream fuel fabrication processes (by elimination of co-milling stages for example) [1]. Such mixed products are likely to produce mixed oxides (MOX) that are homogeneous at the molecular scale, which is a further advantage in MOX fuel performance by avoiding the formation of plutonium-rich grains. Based on the reference European separation processes under development, potential actinide nitrate products are listed in Table 1.

Table 1: Products and processes from advanced actinide separation schemes (TDN = thermal denitration ; ADU = ammonium diuranate ; MDD = modified direct denitration ; WAR = weak acid resin) [2]

Actinides	Key European processes	Potential finishing routes
U	PUREX / Advanced PUREX / COEX / GANEX-1	TDN or ADU
U,Pu	Advanced PUREX / COEX	Oxalate or MDD
U,Pu,Np	Advanced PUREX / COEX	Oxalate or MDD
Am,Cm*	r-SANEX, i-SANEX, 1c-SANEX	Oxalate, gelation, WAR
Am*	EXAm, AMSEL	Oxalate, gelation, WAR
Pu,Np,Am,Cm*	GANEX-2 / EURO-GANEX / CHALMEX	Oxalate
Pu,Np,Am*	Advanced PUREX / COEX with EXAm, AMSEL or future GANEX development	Oxalate

*americium is likely to be re-mixed with uranium to form (U,MA) or (U,TRU) oxide products

Following separation, the actinide nitrate products need to be converted to solid products that can used in fuel fabrication processes, commonly oxide powders [3]. Some of the candidate 'finishing' technologies are also listed in Table 1. Apart from uranium, for the transuranic products the most established conversion process is the oxalate route. This is where the metal nitrate products are precipitated as an oxalate by the addition of oxalic acid, which is filtered and then dried and calcined in furnaces to generate the oxide product [4]. For plutonium, this has been used at the commercial scale in reprocessing plants at La Hague and Sellafield [5] [6]. Studies at the French Alternative Energies and Atomic Energy Commission (CEA) and elsewhere have extended the oxalate route to mixtures of actinides and lanthanides, showing that mixed oxides which are homogeneous at the molecular scale can be generated [7, 4]. Given the industrial experience and significant baseline of R&D, the oxalate route is the most technically mature option and so is considered to be the

This project has received funding from the EURATOM research and training programme 2014-2018 under grant agreement No 755171. The content of this deliverable reflects only the author's view. The European Commission is not responsible for any use that may be made of the information it contains.

'reference' process. Other options may have significant advantages, particularly for the highly radioactive minor actinide (MA) products and should be developed in parallel [8, 9]. An advantage of the oxalate process is that it provides a further decontamination factor (DF) for some fission and corrosion product impurities, except for trivalent lanthanides [10] However, one of the differences in the advanced actinide separation processes compared to conventional reprocessing flowsheets is the introduction of aqueous phase complexing agents in the actinide stripping stages. These complexants are then carried over into the finishing process and thus there is a risk that they (or their degradation products) may perturb the oxalate co-precipitation. Additionally, the oxalate mother liquor (OML) after filtration needs to be recycled into the separation process. This is to minimise actinide losses to waste streams and to reduce the amount of nitric acid usage in the plant (and hence volumes of aqueous effluents). Therefore, strategies are needed to couple the separation and finishing processes, accounting for these issues. Table 2 lists some of these ligands from the European separation processes and Figure 1 provides the structures.
The scope of this paper is to assess the issues caused by the introduction of the aqueous phase complexants in the finishing process with the aim to define where and how the decomposition of the complexant should be performed (see Background section below). The work includes: (a) studies of metal ion oxalate solubilities in the presence of key ligands and the basic degradation product (acetic acid); (b) oxidation of ligands in hot nitric acid and (c) electrochemical oxidation of ligands.

This project has received funding from the EURATOM research and training programme 2014-2018 under grant agreement No 755171. The content of this deliverable reflects only the author's view. The European Commission is not responsible for any use that may be made of the information it contains.

Table 2: Aqueous phase complexants used in actinide stripping stages in key European reference processes (see Figure 1 for structures to complexants)

Process	Complexant
Advanced PUREX	AHA
i-SANEX	Sulphonated-BTP or py-tri-diol
AMSEL	Sulphonated-BTBP
EXAm	TPAEN
EURO-GANEX	AHA with sulphonated-BTP or py-tri-diol

<table>
<tr>
<td> 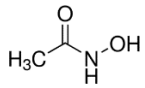
Acetohydroxamic acid
AHA</td>
<td> 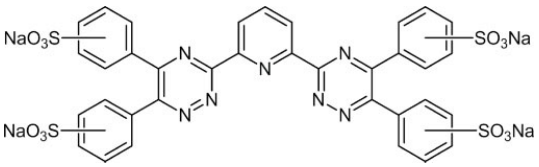
2-6-bis5-6-disulphophenyl-1-2-4-triazin-3-ylpyridine
(s-BTP)</td>
</tr>
<tr>
<td> 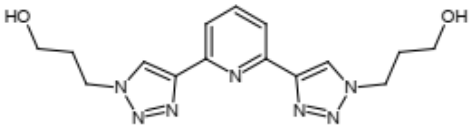
2,6-bis[1-(propan-1-ol)-1,2,3-triazol-4-yl)]pyridine
PyTri-Diol (PTD)</td>
<td> 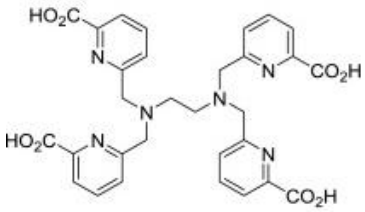
N,N,N’,N’-tetrakis[(6-carboxypyridin-2-yl)methyl]ethylenediamine
TPAEN</td>
</tr>
</table>

Figure 1: Aqueous phase complexants used in actinide stripping stages in key European reference processes including structures, systematic and common names

This project has received funding from the EURATOM research and training programme 2014-2018 under grant agreement No 755171. The content of this deliverable reflects only the author’s view. The European Commission is not responsible for any use that may be made of the information it contains.

BACKGROUND

Specific concerns existing around the behaviour of complexing ligands or their degradation products carried over from the separation process(es) to the finishing process(es) include:

1. Safety, *e.g.* gas generation or explosion risks,
2. Loss of actinides to the OML (increased solubility),
3. Effects on the separation process after recycling OML,
4. Impacts on properties of the mixed actinide oxide products,
5. Incomplete degradation to gases adds to waste volumes.

With respect to points (3) and (5) above, the simplest solution of course is to destroy the ligands simply by boiling in nitric acid in an evaporator. The decomposition of oxalic acid is very effective in hot nitric acid and the kinetics have been reported previously [11]. The hydrolysis of AHA is also well known [12] and forms hydroxylamine nitrate (HAN) and acetic acid in nitric acid. HAN is decomposed to gases by reaction with nitrous acid formed in nitric acid and many papers have studied this sequence of reactions [13]. Acetic acid, however, is known to be quite stable and difficult to decompose to gases [14]. Clearly, the sulphonated-BTP molecule will release sulphur-containing ions into solution that are not compatible with current formulations for nuclear waste glasses (produced in the vitrification process for immobilisation of the high level waste). Whilst the remainder of the sulphonated-BTP and also PTD are 'CHON', nothing is yet known about their decomposition to gases.

Alternative technology may, therefore, be needed to decompose these ligands. Electrochemical oxidation is an obvious candidate technology and previous studies under the European "SACSESS" project [14] evaluated both direct and mediated electrochemical oxidations (DEO, MEO respectively). Significantly better results were obtained with MEO using highly oxidising silver(II) ions as the mediator. Acetic acid was shown to be slow to oxidise by DEO or MEO [14], however a large portion of the acetic acid will be distilled during evaporation and acetic acid is likely to have little effect upon solvent extraction [15]. The impact of recycling acetic acid into the solvent extraction primary extraction stage, will need to be assessed in terms of impacts on solvent extraction and high level waste processes.

Accepting, therefore, that some form(s) of ligand oxidation will be needed, the question arises as to where that stage should be placed within the finishing process flowsheet. There are operational advantages if it can be situated on the OML rather than the feed to the oxalate co-precipitation. The options are illustrated in Figure 2 for a generic flowsheet applicable to Advanced PUREX, i-SANEX, EXAm or EURO-GANEX finishing processes by the oxalate co-conversion route. The solid lines represent the preferred option whereby the

This project has received funding from the EURATOM research and training programme 2014-2018 under grant agreement No 755171. The content of this deliverable reflects only the author's view. The European Commission is not responsible for any use that may be made of the information it contains.

electrochemical ligand oxidation step is on the OML. The dashed lines are the change in process route required if the electrochemical oxidation must be placed before the oxalate precipitation stage. Blue lines represent the aqueous flow, green lines are solid product and amber lines represent the feed reagents needed for specific steps. The main difference between the finishing processes relate to the conditioning step. The Advanced PUREX process reference flowsheet includes a photochemical reactor at this point to co-reduce U(VI) and Pu(III) (and Np if present) to U(IV) and Pu(III) (and Np(IV)) [16]. The i-SANEX or EXAm processes would require the addition of externally generated uranium (IV) to produce a mixed (U,MA) oxide; conditioning would only require acidity adjustment ready for oxalate precipitation. The EURO-GANEX process would also require a co-reduction stage and, if a mixed (U,TRU) product is required, addition of uranium(IV). As these co-finishing processes include mixed actinide oxidation states, counter-cations such as hydrazinium ($N_2H_5^+$) may be needed for charge balancing [4].

The decision on where a ligand oxidation stage should be situated in the flowsheet depends mainly on whether the ligands (or their degradation products) carried over from the solvent extraction process have a detrimental effect on the oxalate co-precipitation process. This can be assessed by studies of the residual metal ion solubilities after oxalate precipitation in the presence of the complexing agents compared to the reference solubilities in the absence of any other species. Any significant increase in metal ion solubility is a potential problem as this will increase actinide losses to the effluent stream (OML)*.

* Impacts on the product morphology or powder properties (e.g. residual carbon concentration) are to be assessed as part of GENIORS Work Package 7.3 (to be reported in Deliverable D7.4).

This project has received funding from the EURATOM research and training programme 2014-2018 under grant agreement No 755171. The content of this deliverable reflects only the author's view. The European Commission is not responsible for any use that may be made of the information it contains.

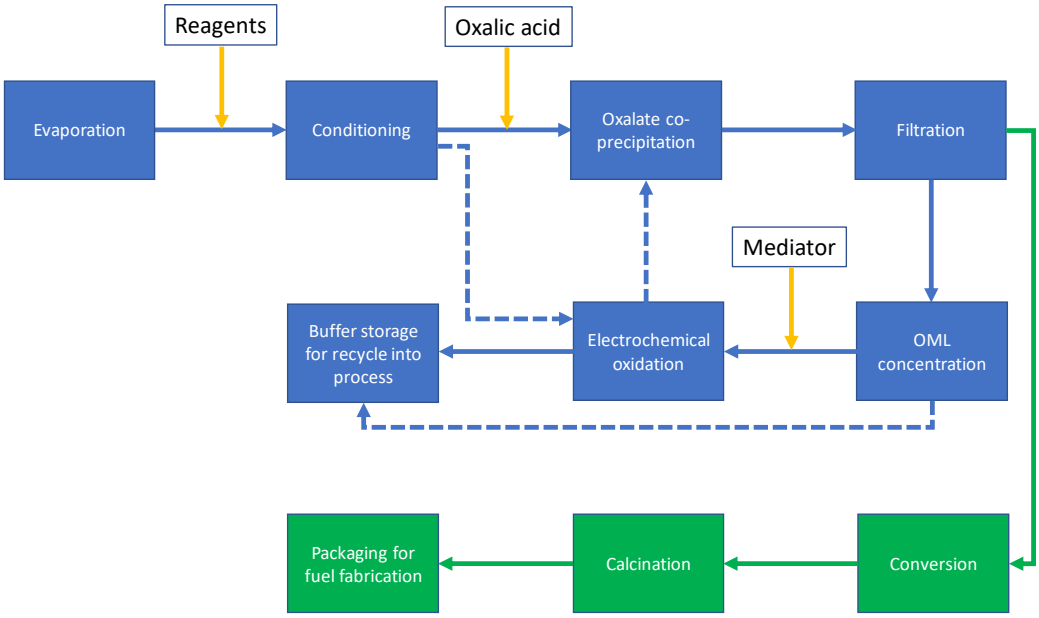

Figure 2: Generic finishing flowsheet for processes based on the oxalate co-precipitation route. The solid lines represent the preferred option whereby the electrochemical ligand oxidation step is on the OML. The dashed lines are the change in process route required if the electrochemical oxidation must be placed before the oxalate co-precipitation step. Blue lines represent the aqueous flow, green lines are solid product and amber lines represent the feed reagents needed for specific steps

This project has received funding from the EURATOM research and training programme 2014-2018 under grant agreement No 755171. The content of this deliverable reflects only the author's view. The European Commission is not responsible for any use that may be made of the information it contains.

AIMS AND OBJECTIVES

This work aims to address two key uncertainties:

- Do complexing ligands effect actinide solubility, which would necessitate oxidation of the ligands prior to oxalate co-precipitation.

As these ligands are known to influence solvent extraction processes, by reducing actinide recovery from the concentrated oxalate mother liquor (CML). Oxidation is necessary, so:

- How can the ligands be oxidised prior to or post oxalate precipitation.

These are assessed by conducting a series of experiments to support the development of a concept flowsheet for the interface between solvent extraction and finishing. By:

- Assessing the impact of key ligands upon oxalate solubility,
- Assessing oxidation of key ligands,
- simulating evaporation in hot nitric acid,
- electrochemical oxidation.

A key constraint of this work is to work at a small scale as some of these ligands currently have limited availability, high cost and are in demand. For these reasons this work focuses on two key areas: oxalate solubility and decomposition studies.

- The effects of AHA/acetic acid and 2,6-bis[1-(propan-1-ol)-1,2,3-triazol-4-yl)]pyridine (known as PyTri-Diol, or PTD) on the solubility of metal ions during oxalate precipitation . Work on the sulphonated BTP, 2-6-bis5-6-disulphophenyl-1-2-4-triazin-3-ylpyridine (herein abbreviated as SO_3-Ph-BTP or s-BTP) is of limited relevance as it is unlikely to be used in future flowsheet development and therefore has not been considered here. This work is also supported by GENIORS deliverable 7.4 on preparation of mixed oxides in a simulated EURO-GANEX product.
- As earlier work under SASCESS has already studied the decomposition of AHA/acetic acid this phase of work will focus on s-BTP and PTD. s-BTP is available and currently not in demand, so was used for an initial starting point in the work. PTD is the key ligand of interest in these studies.

The impact of TPAEN will not be considered in this work, but the approach used in this work could be applied to development of a concept flowsheet in the future.

This project has received funding from the EURATOM research and training programme 2014-2018 under grant agreement No 755171. The content of this deliverable reflects only the author's view. The European Commission is not responsible for any use that may be made of the information it contains.

EFFECTS OF PROCESS LIGANDS ON SOLUBILITIES OF METAL IONS AT THE OXALATE CO-PRECIPITATION STAGE

INTRODUCTION

The insolubility of the plutonium (III,IV) oxalate compounds and their use as precipitating agents in plutonium recovery and purification processes has been well known for decades [17, 18]. Indeed, plutonium (IV) oxalate precipitation followed by calcination remains the standard method for the industrial production of PuO_2 in nuclear fuel reprocessing [3] and modified versions of the oxalate precipitation route are still being investigated for processing Pu, Np, Am and Cm in advanced fuel cycles [19, 20] or from legacy waste streams [21, 22]. The Pu(III) oxalate route, on the other hand, is commonly used for preparing $^{238}PuO_2$ to be used for space power sources [23, 24, 25].

Advanced reprocessing options for future closed fuel cycles often propose to produce mixed actinide products either for reasons of avoiding proliferation concerns that pure plutonium products raise and/or simplifying downstream production of mixed oxide fuels. Examples include the French COEX™ process [26], Advanced PUREX processes [26] and the GANEX process [27] that lead to co-processed (U,Pu), (U,Np,Pu), (Pu,Np,Am,Cm) products respectively in nitric acid. Further, minor actinide (MA) partitioning processes, such as the innovative-SANEX [28] or EXAm [29] processes, that are designed to recover the MA from the PUREX process high active raffinate stream, may be mixed with uranium before conversion to $(U,MA)O_2$ or $(U,Am)O_2$ blanket fuels or targets for accelerator driven systems.

Given the breadth of industrial experience, the oxalate route is often considered the 'reference' process for the conversion (or 'finishing') of these reprocessed actinide nitrate streams to oxide products that are suitable precursors for fuel fabrication [3]. Much effort has been dedicated to the co-precipitation with oxalic acid of U and TRU actinides and their conversion to $(U,TRU)O_2$ solid-solution mixed oxides [4, 7]. In this process, reduction of uranium to the tetravalent oxidation state prior to oxalate precipitation is necessary due to the high solubility of uranyl(VI) oxalate that is the usual uranium product after solvent extraction. However, U(IV) reduces Pu(IV) to Pu(III) and, of course, the MA are also in the +3 oxidation state. Therefore, the factors that affect the co-precipitation of U(IV) and An(III) ions must be thoroughly understood. One key factor is the efficiency of the co-precipitation stage which is evaluated by the residual concentrations of the actinide ions in the oxalate mother liquor (OML) after filtration.

This project has received funding from the EURATOM research and training programme 2014-2018 under grant agreement No 755171. The content of this deliverable reflects only the author's view. The European Commission is not responsible for any use that may be made of the information it contains.

Another question in the development of the oxalate co-precipitation process is that many of the new solvent extraction processes being developed utilise aqueous phase complexants to selectively recover actinides from the organic phase. Whilst complexant-based stripping may have advantages in the separation stages [30], any effects of these complexants on the oxalate precipitation must be understood. Specifically, whether they raise the solubilities of actinides leading to unacceptable losses to the OML, in which case an organics destruction stage would be needed on the concentrated actinide solution prior to oxalate co-precipitation. This would be an undesirable complication compared to a simpler organics destruction stage on the lower activity OML (to enable recycle of nitric acid and trace actinides back into the separation process). The co-precipitation process is illustrated schematically in Figure 2 with the options for the organics destruction stage highlighted.

Here we report new measurements of residual solubilities after oxalate precipitation for Nd(III), Th(IV) and Pu(IV). Nd(III) was selected as a suitable analogue for Am(III) although some confirmatory measurements should eventually be made with Am(III) ions. Th(IV) was used to develop the methods for implementation with Pu in the glove box, as well as of intrinsic interest in the perspective of thorium fuel cycles. The data are compared to literature data and the effects of three key complexants are assessed, these being:

- Aceto-hydroxamic acid (AHA), as used in the Advanced PUREX and EURO-GANEX processes under development [27]
- Acetic acid (AA), which is the hydrolysis product of AHA and likely degradation product of other ligands [31]
- Py-tri-diol (PTD) which is proposed as a selective hydrophilic complexant in the EURO-GANEX and innovative-SANEX processes [32]

This project has received funding from the EURATOM research and training programme 2014-2018 under grant agreement No 755171. The content of this deliverable reflects only the author's view. The European Commission is not responsible for any use that may be made of the information it contains.

BACKGROUND

REVIEW OF EXISTING OXALATE SOLUBILITY DATA

Solubility measurements on Nd(III), Th(IV), Pu(III,IV) and Am(III) oxalates have been compiled from the literature, focusing on the temperature range 20-30 °C to avoid any complications of high temperatures such as post precipitation [33, 34, 35, 36]. This is also the range where most data are available. In order to more easily compare data obtained at varying oxalic acid and nitric acid concentrations, the oxalate ion concentration L^{2-} was calculated, where this is dependent on the dissociation of oxalic acid (a weak acid) in nitric acid (Eq 1,Eq 2). From mass balance considerations (Eq 3) we can derive an expression (Eq 4) for oxalate concentration in terms of the total oxalic acid added, $[L_T]$, and the first and second dissociation stepwise constants of oxalic acid, K' and K" respectively.

$$LH_2 \overset{K'}{\longleftrightarrow} LH^- + H^+ \qquad \text{Eq 1}$$

$$LH^- \overset{K"}{\longleftrightarrow} L^{2-} + H^+ \qquad \text{Eq 2}$$

$$L_T = LH_2 + LH^- + L^{2-} \qquad \text{Eq 3}$$

$$[L^{2-}] = \frac{K'.K"[L_T]}{K'.K" + K'[H^+] + [H^+]^2} \qquad \text{Eq 4}$$

The dissociation constants of oxalic acid, K' and K" have been calculated at 25 °C using ionic strength dependencies of pK_{a1} and pK_{a2} that were reported by Thakur et al. [37]. pK_{a1} and pK_{a2} are described by Eq 5 at 25 °C where respectively Δz^2 is 2 and 4. $\Delta\varepsilon_1$ is 0.076 and $\Delta\varepsilon_2$ is 0.12 in NaCl. Dissociation constants calculated using the Thakur data are compared to values given in the NEA evaluation [38] in Figure 3. There is sufficiently good agreement for our purposes, given the uncertainties in the experimental data at higher ionic strengths and medium effects.

$$pK_{ai} = pK_{ai}^0 - \Delta z^2 D + \Delta\varepsilon_i I \qquad \text{Eq 5}$$

This project has received funding from the EURATOM research and training programme 2014-2018 under grant agreement No 755171. The content of this deliverable reflects only the author's view. The European Commission is not responsible for any use that may be made of the information it contains.

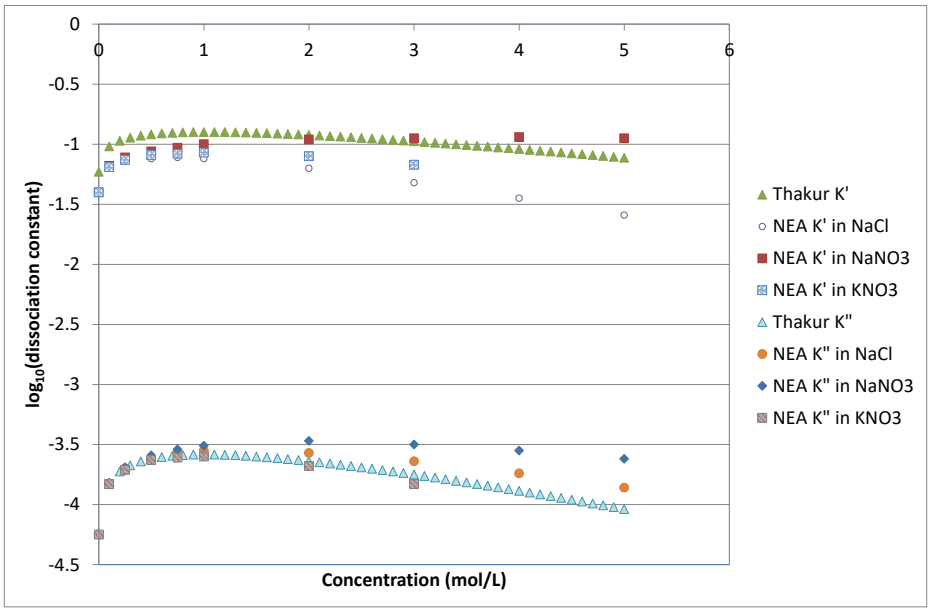

Figure 3: Ionic strength dependence of K' and K"

Given the industrial applications, there are several relevant sources of Pu(IV) oxalate solubility data [39, 18, 40, 41, 42]. Cleveland states that the data of Moskvin are unreliable as equilibrium was not reached in their under-saturation method [18, 43]; hence these data are not included. All data show reasonable agreement although there is a spread which can be attributed to various factors, such as the kinetics of oxalate precipitation, interfering reactions, temperature variations or sampling and analytical errors. Figure 8 ignores a small temperature variation across these data (20–27 °C) but does illustrate the minimum point in Pu(IV) oxalate solubility around $4x10^{-5}$ mol/L (~10 mg/l) in the region of 1×10^{-6} – 1×10^{-7} mol/L oxalate concentration.

Less data has been found in the available literature for thorium(IV) oxalate solubilities; the most relevant source being that of Monson [44]. These data are illustrated in Figure 7 and show lower solubilities than Pu(IV) at higher oxalate concentrations.

There is less plutonium (III) oxalate solubility data to be found in the literature than might be expected; data are illustrated in Figure 4. Perhaps the most useful set is that of Hasilkar et al. [34] who report solubility measurements using under and over-saturation methods with Pu(III) produced by an ascorbic acid reduction. Prior to this work, the report by Porter and Symonds [45] is highly relevant. They investigated Pu(III) oxalate precipitation also with ascorbic acid added to maintain Pu(III) in the working solutions. Solubility increased substantially with nitric acid concentrations over 1 mol/L. Porter and Symonds also provide data on filtrate losses from their precipitation process and testing with Pu-238 solutions

This project has received funding from the EURATOM research and training programme 2014-2018 under grant agreement No 755171. The content of this deliverable reflects only the author's view. The European Commission is not responsible for any use that may be made of the information it contains.

where radiolytic re-oxidation of $Pu(III)_{aq}$ and decomposition of the solid Pu(III) oxalate were problematic. These effects have also been reported for $^{244}Cm(III)$ oxalate [33]. Yarbro et al. [46] took advantage of the hydrolysis of diethyl oxalic acid to generate Pu(III) oxalate. They observed some re-dissolution when precipitates stood for long periods at high temperatures, attributed to re-oxidation to Pu(IV). Data on Pu(III), Am(III) and Cm(III) oxalate solubilities are given by Burney and Porter [33] although the Pu(III) data were obtained from an under-saturation method.

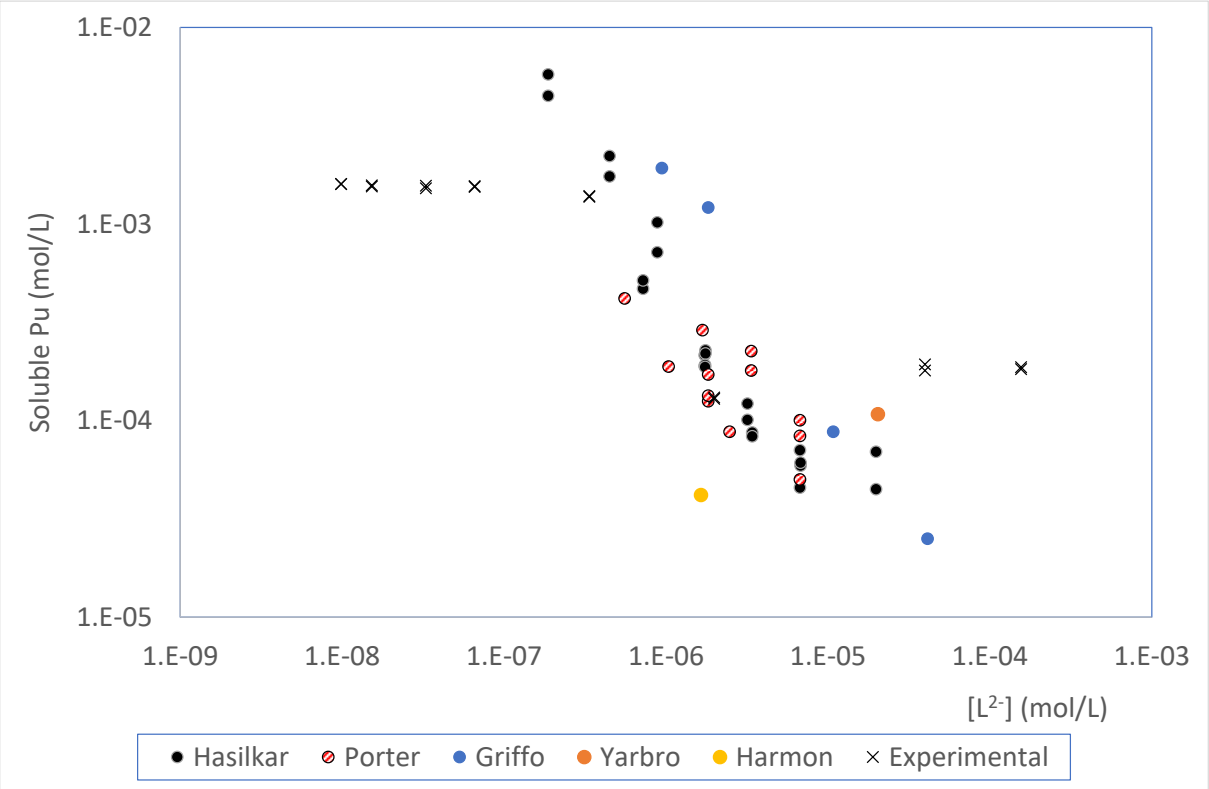

Figure 4: Pu(III) oxalate solubility data [34, 45, 47, 48, 49]

SOLUTION CHEMISTRY (M^{4+} IONS)

In the absence of oxalate, the total An(IV) concentrations present in solubility experiments in acid solutions are assumed to be lower than solubility limits for hydroxides and nitrates. So total An(IV) concentration in solution is given by Eq 6.

$$[An(IV)]_T = [An^{4+}] + \sum_1^j [An(NO_3)_j^{(4-j)+}] + \sum_1^k [An(OH)_k{}^{(4-k)+}] \quad \text{Eq 6}$$

This project has received funding from the EURATOM research and training programme 2014-2018 under grant agreement No 755171. The content of this deliverable reflects only the author's view. The European Commission is not responsible for any use that may be made of the information it contains.

The equilibria describing actinide complexation with nitrate and hydrolysis are given by Eq 7-Eq 8 where β_{Nj} and β_{Hk} are the overall stability constants; therefore, β_{Nj} and β_{Hk} are given by Eq 9-Eq 10. The solubility reaction with oxalate is given by Eq 11 and the solubility product is given by Eq 12.

$$An^{4+} + jNO_3^- \xleftrightarrow{\beta_{Nj}} An(NO_3)_j^{(4-j)+} \quad \text{Eq 7}$$

$$An^{4+} + kH_2O \xleftrightarrow{\beta_{Hk}} An(OH)_k^{(4-k)+} + kH^+ \quad \text{Eq 8}$$

$$\beta_{Nj} = \frac{[An(NO_3)(4-j)+_j]}{[An^{4+}]\,[NO_3^-]^j} \quad \text{Eq 9}$$

$$\beta_{Hk} = \frac{[AnOH(4-k)+_k][H^+]^k}{[An^{4+}]} \quad \text{Eq 10}$$

$$An(C_2O_4)_{2(s)} \xleftrightarrow{K_{sp}} An^{4+}{}_{(aq)} + 2\ C_2O_4^{2-}{}_{(aq)} \quad \text{Eq 11}$$

$$K_{sp} = [An^{4+}]\,[L^{2-}]^2 \quad \text{Eq 12}$$

Considering in the presence of oxalate and nitrate ions, actinide ions (An^{4+}) form complexes in solution, the overall solubility will be the sum of all solution species likely to be present, *i.e.* the sum of free metal ion plus oxalate, nitrate and hydrolysed complexes, Eq 13.

$$S_{An} = [An^{4+}] + \sum_1^i [AnL_i^{(4-2i)+}] + \sum_1^j [An(NO_3)_j^{(4-j)+}] + \sum_1^k [An(OH)_k^{(4-k)+}] \quad \text{Eq 13}$$

The equilibria describing actinide ion complexation with oxalate anions is given by Eq 14 where β_i are the overall stability constants given by Eq 15.

$$An^{4+} + iL^{2-} \xleftrightarrow{\beta_i} AnL_i^{(4-2i)+} \quad \text{Eq 14}$$

$$\beta_i = \frac{[AnL(4-2i)+_i]}{[An^{4+}]\,[L^{2-}]^i} \quad \text{Eq 15}$$

This project has received funding from the EURATOM research and training programme 2014-2018 under grant agreement No 755171. The content of this deliverable reflects only the author's view. The European Commission is not responsible for any use that may be made of the information it contains.

A full description of the solution chemistry, therefore, requires the thermodynamic equilibrium constants for these reactions to be known as functions of ionic strength. For example, Berg *et al.* [43] have reported equations for nitrate complexation using Specific Ion Interaction Theory (SIT) given by Eq 16 where for j = 1-2, Δz^2 is 8 and 14 respectively; $\log\beta_1^0$ = 2.12 ±0.2; $\log\beta_2^0$ = 3.66 ±0.4; I is the ionic strength (molal); D is the Debye-Hückel term and ε represents ion interaction coefficients where $\Delta\varepsilon_1$ = 0.17 ±0.02 and $\Delta\varepsilon_2$ = 0.36 ±0.03[15]. Similarly, the hydrolysis constants (K_1 and K_2) are given in Eq 17 where for k = 1-2, Δz^2 is 6 and 10 respectively; $\log\beta^\circ_1$ = 0.60, $\log\beta^\circ_2$ = 0.60, $\Delta\varepsilon_1$ = 0.18 and $\Delta\varepsilon_2$ = 0.24 for the respective hydrolysis reactions (in $HClO_4$) [50, 51].

$$log_{10}\,\beta_{Nj} = log_{10}\,\beta^0_{Nj} - \Delta z^2 D + \Delta\varepsilon_i I \qquad \textbf{Eq 16}$$

$$log_{10}\,\beta_{Hk} = log_{10}\,\beta^0_{Hk} - \Delta z^2 D + \Delta\varepsilon_i I \qquad \textbf{Eq 17}$$

Substituting for the concentrations of species in Eq 13 from the equilibrium reactions described by Eq 9,Eq 10,Eq 15 will lead to an equation for the total metal ion solubility that describes An(IV) oxalate-nitrate systems in terms of all the species likely to be present assuming the actinide oxalates are the solubility limiting phase. For the present, to simplify the system, the nitrate and hydrolysed complexes are neglected in Eq 18.

$$S_{An(IV)} = \frac{K_{sp}}{[L]^2}\{1 + \beta_1[L] + \beta_2[L]^2 + \beta_3[L]^3\} \qquad \textbf{Eq 18}$$

Therefore, with Eq 4 and Eq 18 we have the means to determine either K_{sp} from oxalate solubility experiments or, if K_{sp} is known to us, to predict total solubilities after precipitation. However, ionic strength dependent values of $\beta_{1\text{-}3}$ for Pu(IV) oxalate complexes have not been found in the literature.

Similar arguments can be made for the trivalent metal ions remembering that the solubility equation is given by Eq 19 and Eq 20.

$$An_2(C_2O_4)_{3(s)} \xleftrightarrow{K_{sp}} 2An^{3+}{}_{(aq)} + 3\ C_2O_4{}^{2-}{}_{(aq)} \qquad \textbf{Eq 19}$$

This project has received funding from the EURATOM research and training programme 2014-2018 under grant agreement No 755171. The content of this deliverable reflects only the author's view. The European Commission is not responsible for any use that may be made of the information it contains.

Eq 20

$$S_{M(III)} = \sqrt{\frac{K_{sp}}{[L]^3}}\{1 + \beta_1[L] + \beta_2[L]^2 + \beta_3[L]^3\}$$

EXPERIMENTAL METHODS

The same method was used throughout the oxalate solubility studies. Experiments were carried out across both non-active and active laboratories and utilised both fumehood and plutonium active gloveboxes. The molarity of the metal under investigation was kept constant in each experiment. Initially the total volume for each reaction was 10 mL and all experiments were completed in duplicate, but this was scaled down to 2 mL for the PTD experiments to reduce the amount of ligand required to complete the whole series of experiments. Further, due to the limited availability of PTD an experimental design study was completed by NNL's Decision Science team to optimise the number of experiments required whilst still giving the same level of information required. The experimental design included factorial points, bounding the area under investigation; centre points, repeated in triplicate, to understand repeatability of the experiments and highlight any potential systematic errors and axial points get a better understanding of how the outputs vary over a range of [HNO_3] and [oxalic acid]. Full details are provided in reference [52].

A Radley Carousel 12 plus reaction station (Figure 5) reaction vessel was used to carry out the precipitation experiments and was maintained at a constant temperature of 25 °C. For each experiment, a predetermined amount of metal nitrate stock was added to each reaction vessel followed by the desired quantities of nitric acid, ultra pure water and ligand (if required). For the 10 mL tests, a magnetic stirrer was added to each reaction tube and the stirrer plate was set to 500 rpm. For the 2 mL tests, an Eppendorf Thermomixer C shaker (Figure 6) was used because a magnetic stirrer was not suitable due the size of the vials. The shaker was also set to 500 rpm at 25 °C. Once the temperature had stabilised, the required amount of oxalic acid was added, and the solution was left to stir. For the 10 ml tests, the stirrer was switched off at 4 and 6 hours and the precipitate allowed to settle. For the 2 ml; tests, the shaker was stopped at 5 hours. In both instances, aliquots of the supernatant were taken and filtered using a Sartorius Vivaspin 500 centrifugal concentrator before a series of dilution factors were applied in order to conduct ICP-MS analysis. These results provide the information to determine the concentration of metal in solution.

This project has received funding from the EURATOM research and training programme 2014-2018 under grant agreement No 755171. The content of this deliverable reflects only the author's view. The European Commission is not responsible for any use that may be made of the information it contains.

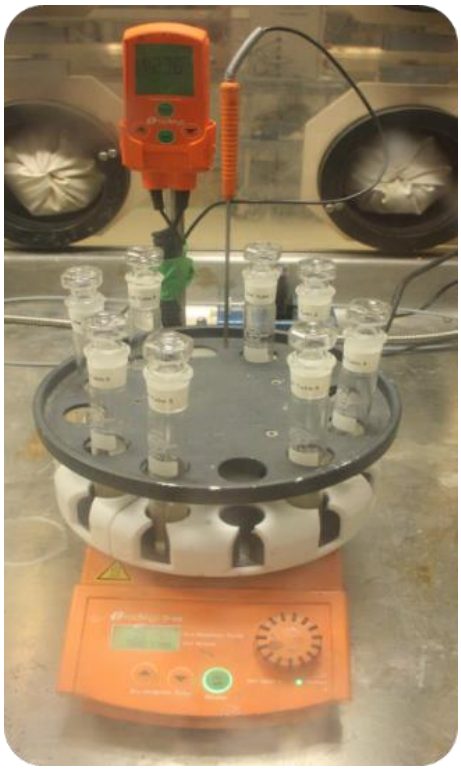

Figure 5. Experimental set up for the 10 ml scale using the Radley Carousel.

Figure 6. Experimental set up for 2 ml scale using the Eppendorf Thermomixer C shaker.

This project has received funding from the EURATOM research and training programme 2014-2018 under grant agreement No 755171. The content of this deliverable reflects only the author's view. The European Commission is not responsible for any use that may be made of the information it contains.

RESULTS AND DISCUSSION

THORIUM (IV)

The experimental matrix for the Th(IV) studies is shown in Table 3 and data are illustrated in Figure 7. It is apparent that the solubilities of Th(IV) oxalate determined in the present work are significantly lower than those of Monson [44]. These new data are considered meaningful given the agreement with our Pu(IV) data with the literature below and that experimental issues such as poor phase separation are more likely to result in erroneously higher solubilities. Moreover, two batches of experiments were carried out at different times separated by a year. Each data point is the average of at least two samples taken at different digestion times and duplicate precipitations were made for each datapoint. Very good agreement was obtained between experiments and the dataset is highly self-consistent. The minimum solubility is at a higher oxalate concentration than Pu(IV) due to lower complexation constants of Th(IV) with oxalate than Pu(IV). There are no effects on solubility observed with either 0.05 mol/l acetic acid or AHA present in the initial solution.

This project has received funding from the EURATOM research and training programme 2014-2018 under grant agreement No 755171. The content of this deliverable reflects only the author's view. The European Commission is not responsible for any use that may be made of the information it contains.

Table 3. Experimental matrix of conditions used for Th(IV) studies.

Experiment No	[HNO_3] (mol/l)	[Oxalic Acid] (mol/l)	[$Th(NO_3)_4$] (mol/l)	[Ligand] (mol/l)
1	0.2	0.1	0.00228	0.05
2	0.2	0.2	0.00228	0.05
3	0.3	0.01	0.00228	0
4	0.3	0.03	0.00228	0.05
5	0.3	0.1	0.00228	0
6	0.3	0.15	0.00228	0
7	0.3	0.2	0.00228	0
8	1	0.01	0.00228	0
9	1	0.03	0.00228	0
10	1	0.1	0.00228	0.05
11	1	0.15	0.00228	0.05
12	1	0.2	0.00228	0
13	3	0.01	0.00228	0.05
14	3	0.03	0.00228	0.05
15	3	0.1	0.00228	0
16	3	0.15	0.00228	0.05
17	3	0.2	0.00228	0
18	3	0.25	0.00228	0.05
19	3	0.3	0.00228	0
28	0.1	0.3	0.00228	0.05
29	0.1	0.4	0.00228	0

This project has received funding from the EURATOM research and training programme 2014-2018 under grant agreement No 755171. The content of this deliverable reflects only the author's view. The European Commission is not responsible for any use that may be made of the information it contains.

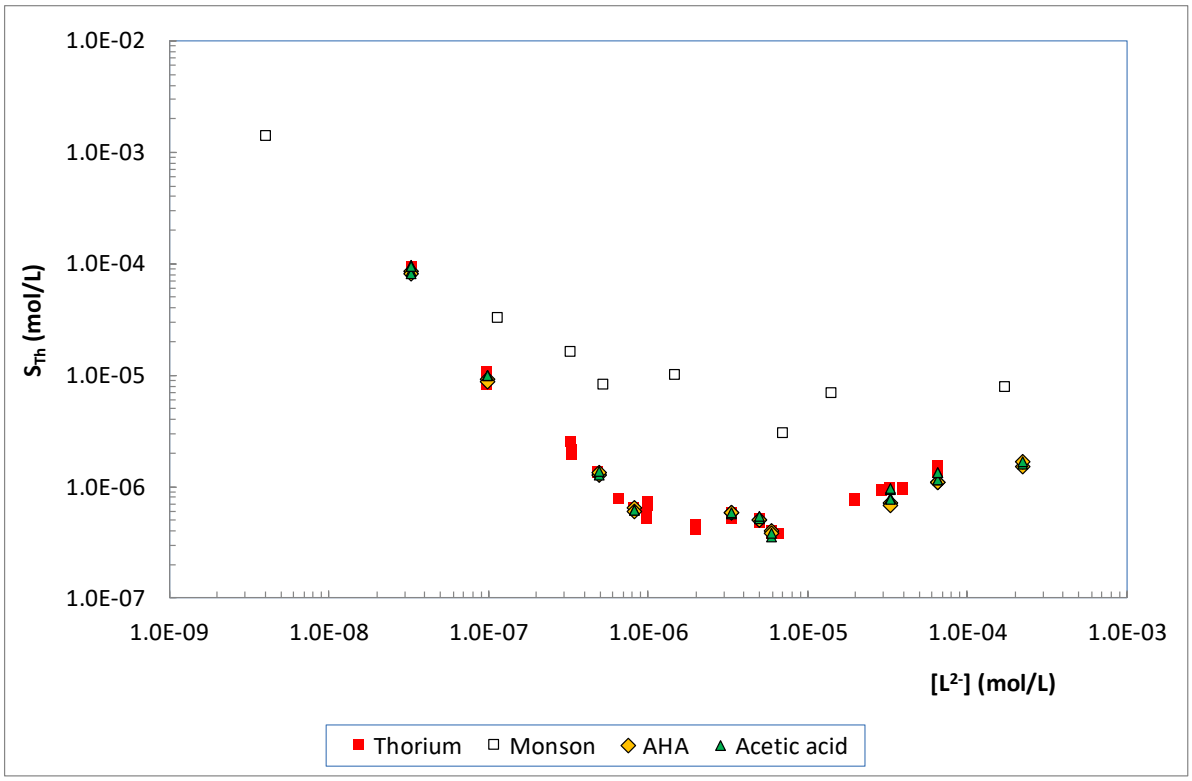

Figure 7: Th(IV) oxalate solubility results compared to literature (Monson, [44]) and with acetic acid and AHA present in solution

This project has received funding from the EURATOM research and training programme 2014-2018 under grant agreement No 755171. The content of this deliverable reflects only the author's view. The European Commission is not responsible for any use that may be made of the information it contains.

PLUTONIUM (IV)

Following the thorium studies, a series of similar experiments were carried out to determine the solubility of Pu(IV). The experimental conditions used were the same as those used as part of the thorium matrix, but also some additional experiments were completed to understand the effect of changing the ligand concentration (Table 4).

Table 4. Additional experimental conditions investigated with Pu(IV).

Experiment No	[HNO_3] (mol/l)	[Oxalic Acid] (mol/l)	[$Pu(NO_3)_4$] (mol/l)	[Ligand] (mol/l)
1	0.1	0.3	0.00228	0.3
2	0.3	0.03	0.00228	0.3
3	2	0.1	0.00228	0.3
4	3	0.01	0.00228	0.3
5	0.1	0.3	0.00228	0.5
6	0.3	0.03	0.00228	0.5
7	2	0.1	0.00228	0.5
8	3	0.01	0.00228	0.5

This project has received funding from the EURATOM research and training programme 2014-2018 under grant agreement No 755171. The content of this deliverable reflects only the author's view. The European Commission is not responsible for any use that may be made of the information it contains.

Data from various literature sources related to Pu(IV) solubility are illustrated in Figure 8. It is apparent that there is some spread in the data, probably due to post-precipitation, temperature differences and sampling issues, although plutonium redox chemistry may also be a factor particularly at low acidity where Pu(IV) disproportionates. Nevertheless, the trend toward the minimum solubility point at $[L^{2-}]$ *ca.* 3×10^{-7} mol/l is clear.

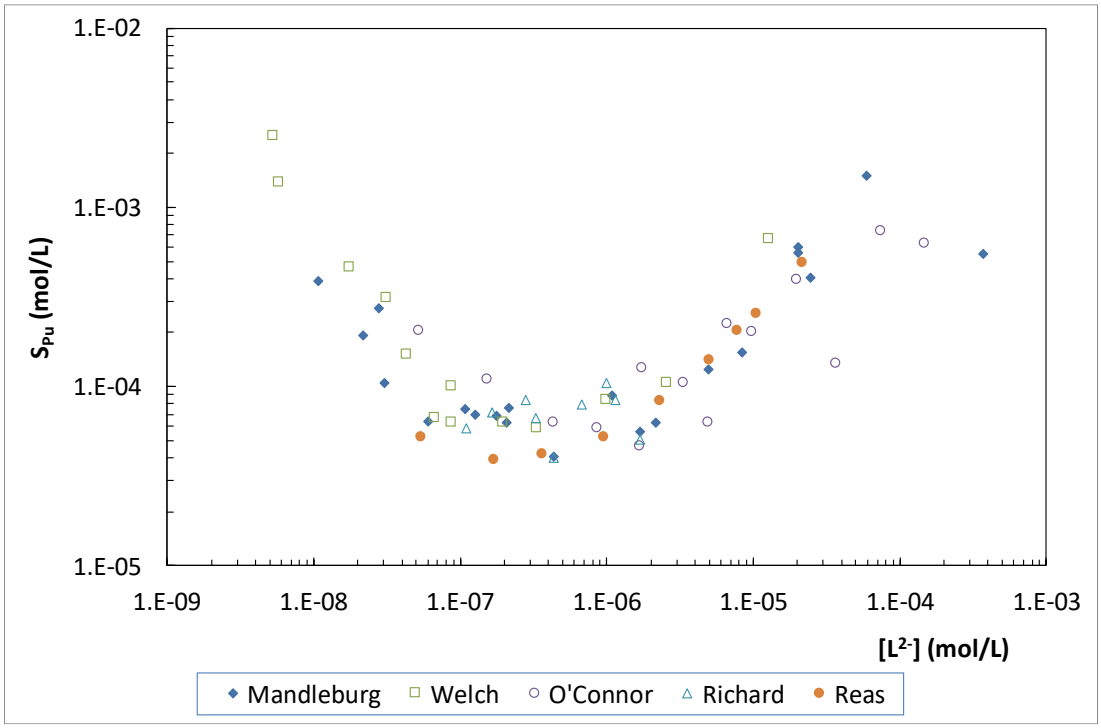

Figure 8: Pu(IV) oxalate solubilities, literature data (20-30 °C).

This project has received funding from the EURATOM research and training programme 2014-2018 under grant agreement No 755171. The content of this deliverable reflects only the author's view. The European Commission is not responsible for any use that may be made of the information it contains.

New Pu(IV) experimental data are compared to the Mandleburg [39] and Reas literature data in Figure 9 and good agreement is observed. The minimum solubility is higher and at a lower oxalate concentration than Th(IV) due to higher complexation constants of Pu(IV) with oxalate than Th(IV).

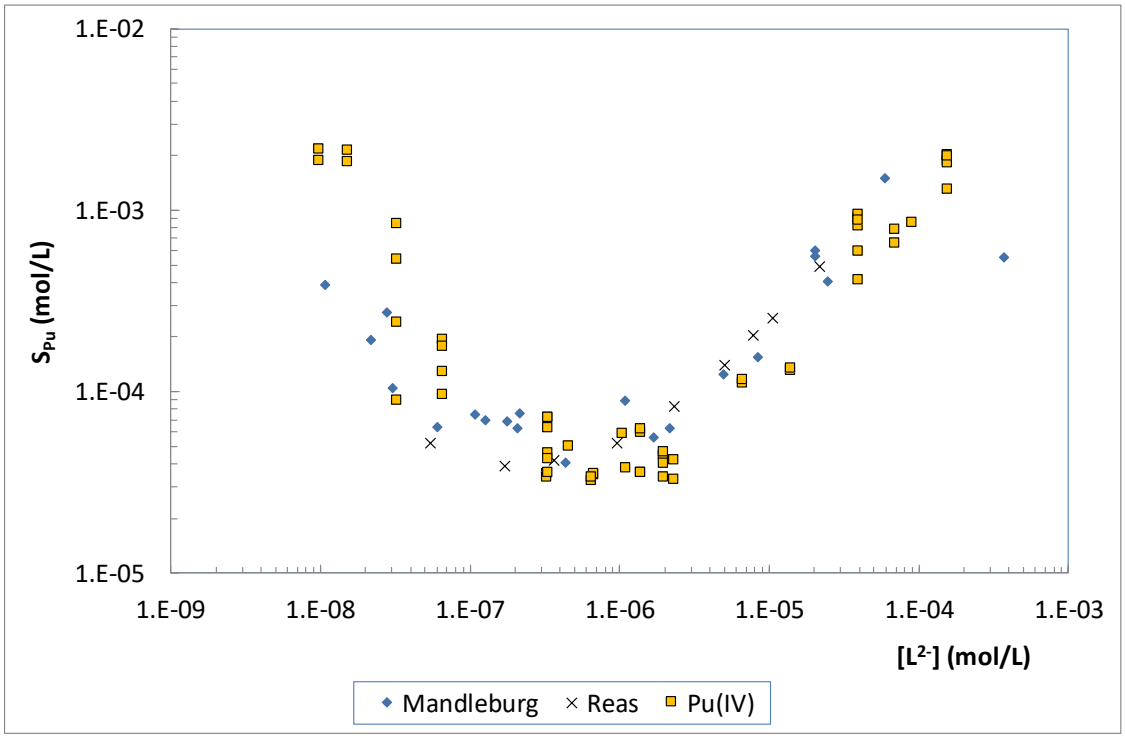

Figure 9: Pu(IV) oxalate solubilities, comparison of experimental (25 °C) and literature data (20-30 °C)

This project has received funding from the EURATOM research and training programme 2014-2018 under grant agreement No 755171. The content of this deliverable reflects only the author's view. The European Commission is not responsible for any use that may be made of the information it contains.

The effects of 0.05 to 0.5 mol/l acetic acid and AHA on the measured Pu(IV) oxalate solubilities are shown in Figure 10 (compared to our Pu(IV) data). There are only small effects on the minimum solubility with 0.05 mol/l acetic acid and AHA. 0.05 mol/l acetic acid appears to decrease the soluble Pu(IV), perhaps due to a buffering effect of the acetate whereas AHA raises it slightly from 10-20 mg/l Pu. There are limited effects at the higher concentration (0.5 mol/l) range and fall within the spread of data observed for Pu(IV) solubility.

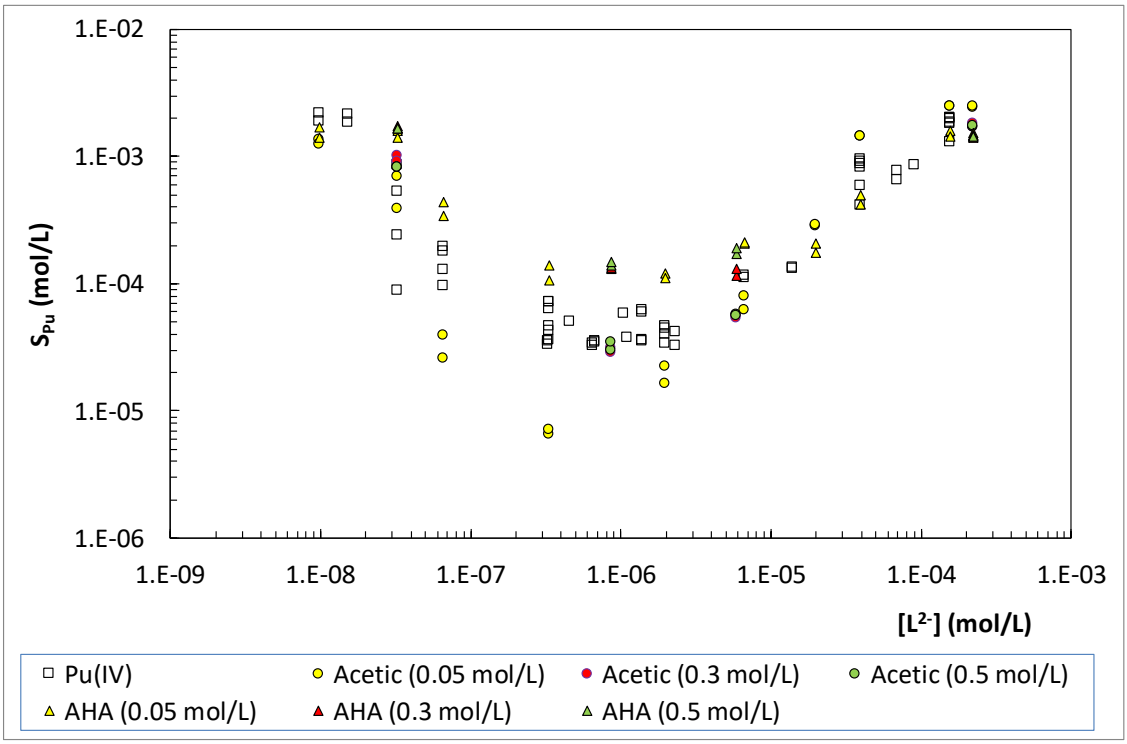

Figure 10: Effect of AHA and acetic acid on Pu(IV) oxalate solubilities (25 °C).

This project has received funding from the EURATOM research and training programme 2014-2018 under grant agreement No 755171. The content of this deliverable reflects only the author's view. The European Commission is not responsible for any use that may be made of the information it contains.

NEODYMIUM (III)

In order to study the effects of PTD on the solubility of metals, it was necessary to scale down the experimental volume from 10 to 2 ml to reduce the amount of ligand required. Previous results were collected for Nd(III) at an increased volume and as such it was necessary to conduct repeat tests at 2 ml to compare the results. This confirmed there were no issues caused due to scaling and consistency in the data was still obtained. Another tool that was utilised to determine the experimental matrix but still ensure fair comparison was achieved between all the different metal studies, was statistical down selection. This reduced the number of tests needed but produced a data set that is comparable across all the results collected previously.

Data obtained from the Nd studies are included in Figure 11. Good agreement is observed between the batches of experiments carried out and against those conducted at different times. Overall, there seems to be very minimal effect of PTD on the solubility. During these studies, some experiments were measured after only 1 hour of digestion compared to the intended 5 hour run. These data are named ‘ICP-OES’ in the plot below and show slightly different behaviour. As a result of this, the change in conditions was not considered conducive to these investigations and would cause discrepancies between data sets and the 5 hour experiments were resumed.

This project has received funding from the EURATOM research and training programme 2014-2018 under grant agreement No 755171. The content of this deliverable reflects only the author’s view. The European Commission is not responsible for any use that may be made of the information it contains.

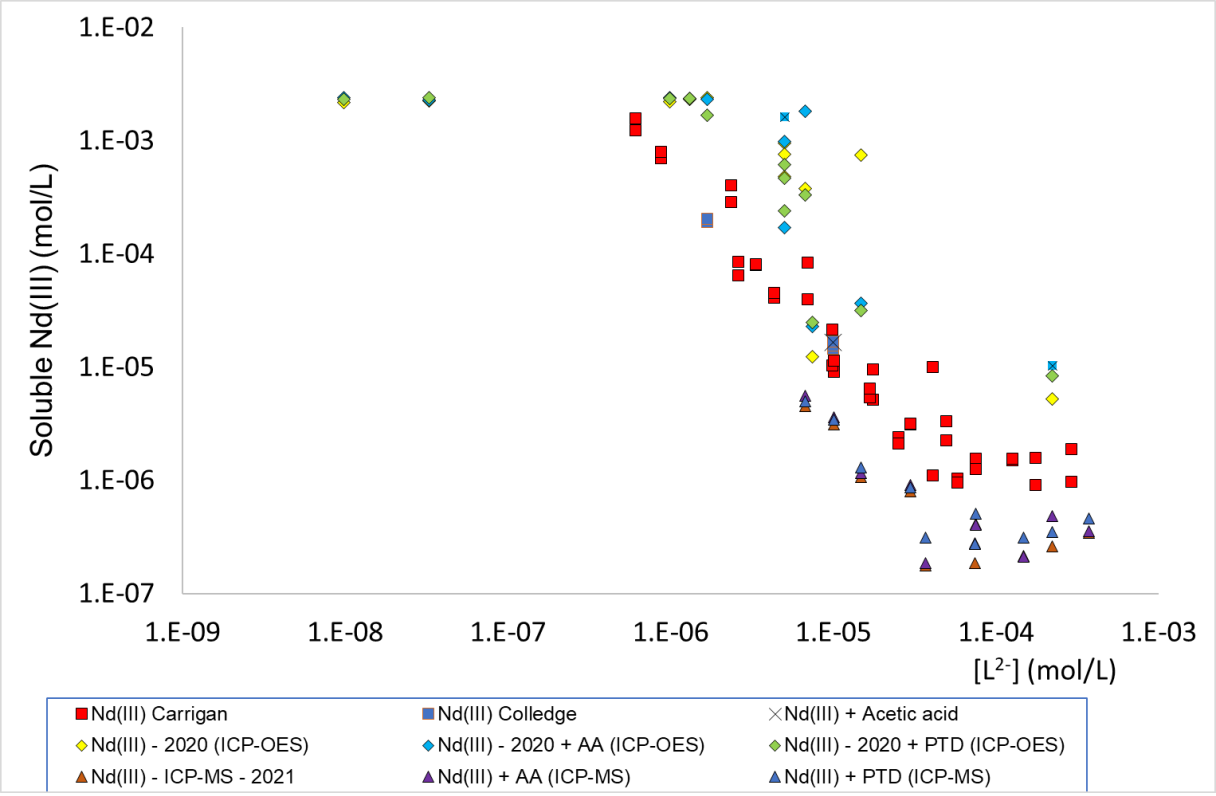

Figure 11. Nd(III) oxalate solubilities, comparison of new experimental data with previous NNL data and the effects of AA and PTD on Nd(III) solubility (25 °C).

This project has received funding from the EURATOM research and training programme 2014-2018 under grant agreement No 755171. The content of this deliverable reflects only the author's view. The European Commission is not responsible for any use that may be made of the information it contains.

SOLUBILITY STUDIES SUMMARY

In conclusion, the method developed and used here for determining the solubility of different metals has shown to generate consistent and reliable results. This is true in comparison to existing literature data and within independent batches of NNL experiments carried out at different times. It is clear from the results that it is possible to create 'ideal conditions' by varying the nitric and oxalic acid concentrations in order to control the solubility of different metals. This is achieved as the concentration in HNO_3 decreases and the oxalic acid concentration increases, a dip in solubility is observed. Therefore, creating the most optimal conditions for reduced solubility. Overall, investigations into the different ligands show they have very little if no effects on the solubility of Pu(IV), Th(IV) and Nd(III) oxalates.

Following on from this work, the next phase will focus on understanding the solubility of Pu(III) and Am(III) oxalates and the effects of PTD on Pu(IV) and Pu(III) oxalates.

This project has received funding from the EURATOM research and training programme 2014-2018 under grant agreement No 755171. The content of this deliverable reflects only the author's view. The European Commission is not responsible for any use that may be made of the information it contains.

EFFECTS OF HOT NITRIC ACID ON DECOMPOSITION OF PROCESS LIGANDS

This work is a simple series of experiments that are relevant to understanding the behaviour of s-BTP and PTD under evaporators used to concentrate wastes prior to recovery of actinides by solvent extraction.

EXPERIMENTAL:

DECOMPOSITION OF LIGANDS IN HOT NITRIC ACID

The first stage of the work involved boiling either s-BTP or PTD in a range of HNO_3 concentrations. s-BTP and PTD were obtained from Technocomm Ltd, UK. 10 ml stocks of 100 g/l s-BTP and PTD were made up by dissolution in demineralised water. A series of nitric acid solutions were also made up from 2 to 15.8 mol/l using volumetric glassware and AR nitric acid (Fishers Scientific). 50 ml of the required acid was measured out using a 50 ml volumetric flask with 0.5 ml of 100 g/l ligand added to the flask. The list of experiments are detailed in Table 5. The large central neck on the round bottom flask was connected to a 525 mm condenser and the side arm used for sample flasks using a 1/8" PVDF tube, adapter with valve and syringe to allow sampling. The round bottom flasks were heated with a hotplate with a five position heating block (Radley starfish). The experimental set up is shown in Figure 12. The condensers were cooled to *ca*. 7 ºC using a chiller recirculatory and the hotplate set to allow gentle reflux. 3-5 ml samples were taken at approximately 0, 1, 2, 4 and 20 hrs, where allowable, some experiments were additionally sampled at around 6 hrs. All samples were analysed by total carbon (combustion), and UV-Vis spectroscopy.

This project has received funding from the EURATOM research and training programme 2014-2018 under grant agreement No 755171. The content of this deliverable reflects only the author's view. The European Commission is not responsible for any use that may be made of the information it contains.

Table 5. List of boiling experiments.

[HNO_3] (mol/l)	[s-BTP] (g/l)	Experiment name	[PTD] (g/l)	Experiment name
2	1	BE-2M-sBTP	1	BE-2M-PTD
4	1	BE-4M-sBTP	1	BE-4M-PTD
6	1	BE-6M-sBTP	1	BE-6M-PTD
8	1	BE-8M-sBTP	1	BE-8M-PTD
10	1	BE-10M-sBTP	1	BE-10M-PTD
12	1	BE-12M-sBTP	1	BE-12M-PTD
14	1	BE-14M-sBTP	1	BE-14M-PTD
15.8	-	-	1	BE-15.8M-PTD

Figure 12. Set up of equipment for Boiling experiments.

This project has received funding from the EURATOM research and training programme 2014-2018 under grant agreement No 755171. The content of this deliverable reflects only the author's view. The European Commission is not responsible for any use that may be made of the information it contains.

TOTAL CARBON ANALYSIS (TOC)

Total carbon analysis was carried out using a Shimadzu TOC-L in total carbon analysis mode. This is thermal composition carried out at 780 °C on a platinum catalyst using an injection volume of 50 µl (two or three replicates). Calibration was carried out using standard sodium phthalate solutions. All samples were diluted to DF10 with demineralised water before analysis.

UV-VIS SPECTROSCOPY

All UV-Vis spectra were recorded using a Zeiss MCS601 spectrometer with halogen lamp, fibre optic cables and a 10 mm path length cuvette. UV-Vis analysis of s-BTP and PTD was carried out using an iron(II) complexation method as published by Treister et al [53] and further developed to measure s-BTP concentration by Herdzik-Koniecko et al. [54].

Calibration curves on the UV-Vis spectrometer were made with a series of dilutions from the 100 g/l s-BTP and PTD stock solutions. A range of concentrations over 10 samples were prepared in 10 ml of matrix. The matrix was composed of 3×10^{-4} mol/l $Fe(NO_3)_3$, 0.015 mol/l HNO_3, 0.1 mol/l hydroxylamine hydrochloride in a 1 mol/l acetate buffer at pH 4.5. The matrix was made by preparing an acetate buffer by dissolution of 49.9 g sodium acetate (trihydrate) in 700 ml of demineralised water, pH checked using a combined pH electrode, adjusted as necessary using up to 38.7 g acetic acid and made up to pH 4.5 at 1 L using demineralised water. To 500 ml of the acetate buffer 0.121 g iron(III) nitrate, 6.95 g hydroxylamine hydrochloride and 0.096 ml 69 % nitric acid were dissolved and resulting solution made up to 1 L with acetate buffer.

s-BTP calibration curves were prepared in the range 2-50 µmol/l s-BTP. These were prepared by producing three working s-BTP solutions; named A, B and C. Dilution A consisted of 0.1 ml into 9.9 ml demineralised water, dilution B of 0.1 ml into 19.9 ml demineralised water and dilution C, 0.1 ml into 49.9 ml demineralised water. 0.1 to 0.5 ml of dilutions A, B and C were added to 10 ml matrix. Boiling experiment samples were analysed by addition of 0.2 ml boiling test samples into 10 ml matrix.

PTD calibration curves were prepared in the range 6-150 µmol/l PTD. These were prepared by producing three working PTD solutions; named A, B and C. Dilution A was 0.1 ml into 10 ml demineralised water, dilution B, 0.1 ml into 20 ml demineralised water and dilution C, 0.1 ml into 50 ml demineralised water. 0.1 to 0.5 ml of dilutions A, B and C were added to 10 ml matrix. Boiling experiment samples were analysed by addition of 0.3 ml boiling test

This project has received funding from the EURATOM research and training programme 2014-2018 under grant agreement No 755171. The content of this deliverable reflects only the author's view. The European Commission is not responsible for any use that may be made of the information it contains.

samples into 10 ml matrix. The complex formation for the PTD was found to be slower than the s-BTP and required a >10 min development time before measurement.

RESULTS

IRON(II) S-BTP UV-VIS CALIBRATION

The absorption spectra, baseline corrected to 800 nm, of the iron(II)/s-BTP complex in hydroxylamine buffer matrix are shown in Figure 13. The absorbance at 471 nm was used to produce a good Beer Lambert calibration plot, shown in Figure 14.

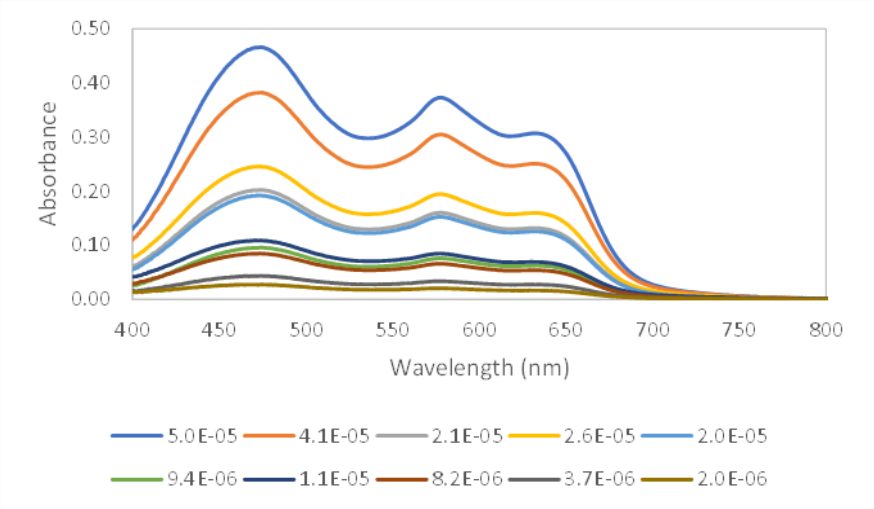

Figure 13: Baseline corrected absorption spectra of the Fe(II)/s-BTP complex. s-BTP concentration (in µmol/l) shown in legend. Path length: 10 mm.

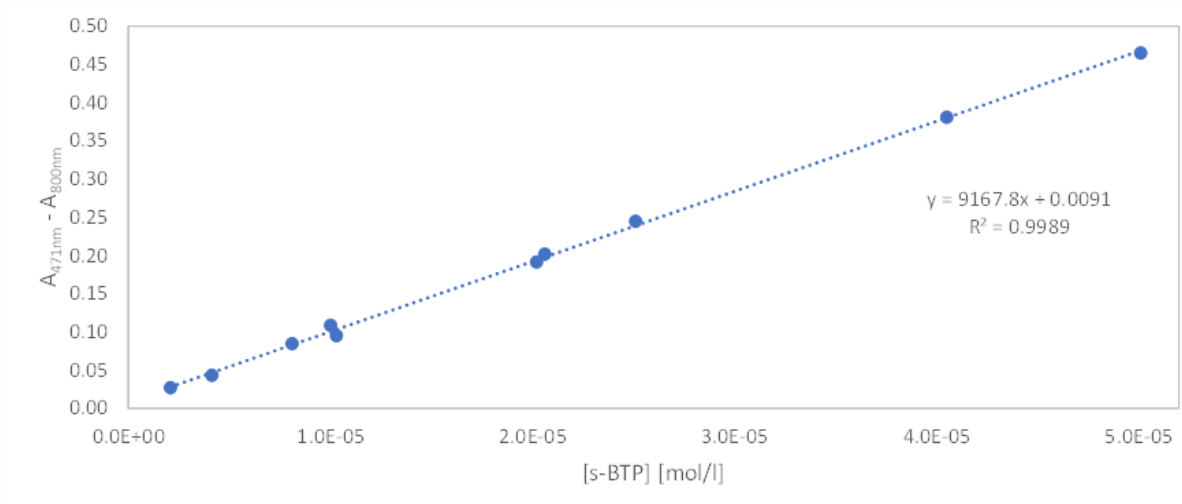

This project has received funding from the EURATOM research and training programme 2014-2018 under grant agreement No 755171. The content of this deliverable reflects only the author's view. The European Commission is not responsible for any use that may be made of the information it contains.

Figure 14: Beer Lambert plot of the Fe(II)/s-BTP complex at 471 nm.

IRON(II) PTD UV-VIS CALIBRATION

As PTD shows similar binding characteristics with s-BTP, it was proposed to use the same matrix-based solution route to quantify the concentration of PTD in solution. Initial calibration attempts showed that the PTD did successfully form a coloured complex with the iron(II), with a maxima at 438 nm, but showed a high variability in absorbance within similar concentration solutions. The calibration plot was run with samples aged >10 min, but a fixed colour development time was not used at this stage. Later experiments showed that there is an increase in the absorption over time, Figure 15, however the calibration was not repeated as the maximum absorbance is reached after *ca.*10 mins. The absorption spectra, baseline corrected to 550 nm, of the iron(II)/PTD complex in hydroxylamine buffer matrix are shown in Figure 16. The absorbance values were extracted at 438 nm and produced a good Beer Lambert calibration plot, shown in Figure 17.

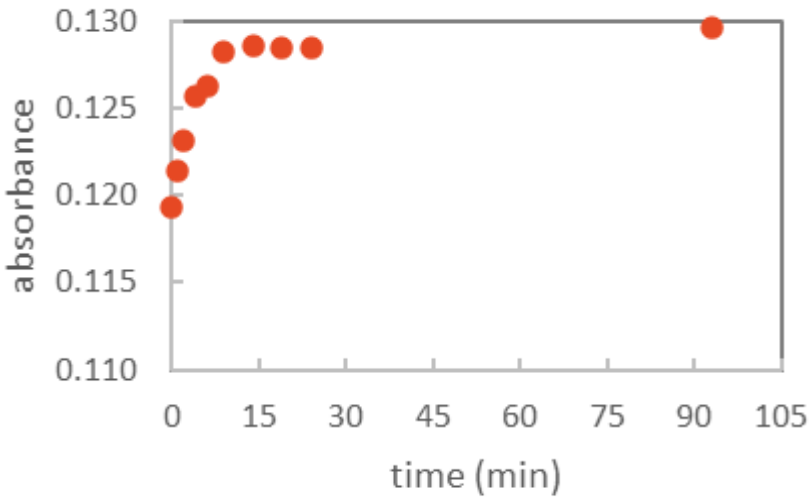

Figure 15: PTD-Fe(II) complex formation over time at 1.52 x10^{-3} mol/L PTD

This project has received funding from the EURATOM research and training programme 2014-2018 under grant agreement No 755171. The content of this deliverable reflects only the author's view. The European Commission is not responsible for any use that may be made of the information it contains.

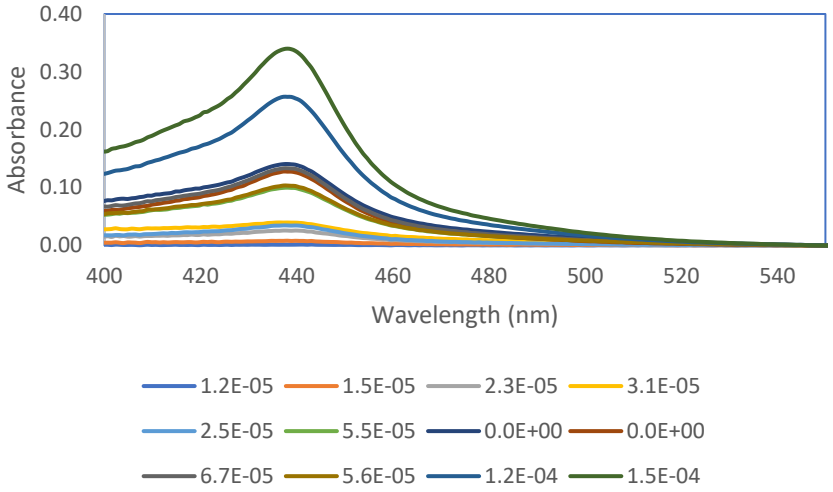

Figure 16: Baseline corrected absorption spectra of the Fe(II)/PTD complex. PTD concentration (mol/l) shown in legend. Path length: 10 mm

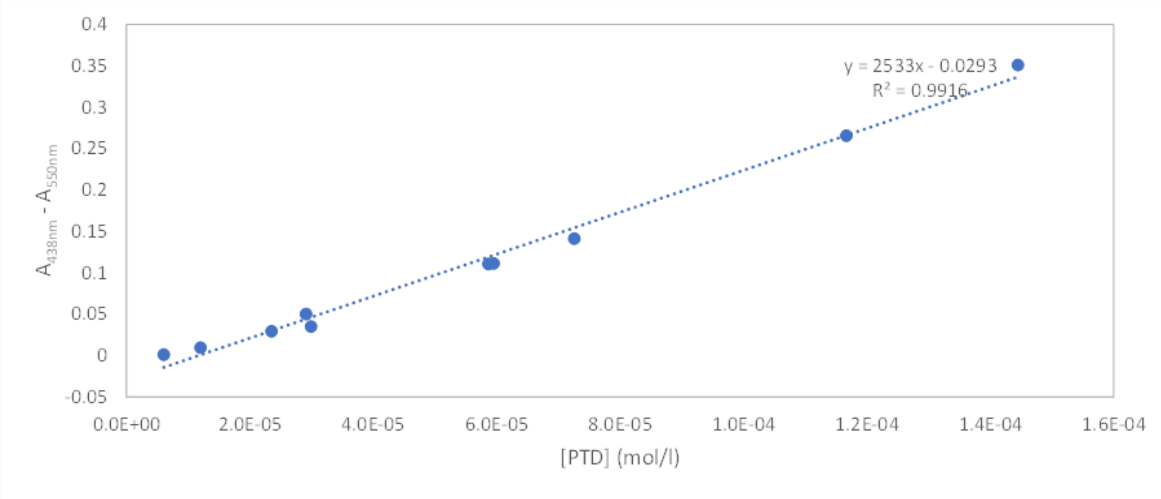

Figure 17: Beer-Lambert plot of absorbance of the Fe(II)/PTD complex at 438 nm

This project has received funding from the EURATOM research and training programme 2014-2018 under grant agreement No 755171. The content of this deliverable reflects only the author's view. The European Commission is not responsible for any use that may be made of the information it contains.

S-BTP DECOMPOSITION OF LIGANDS IN HOT NITRIC ACID

The final samples (>20 hours reflux) for the 1 g/l s-BTP solutions are shown to be discoloured in nitric acid concentrations above 8 mol/l acid, Figure 18. No precipitate was observed either throughout the experiment, or in any sample taken.

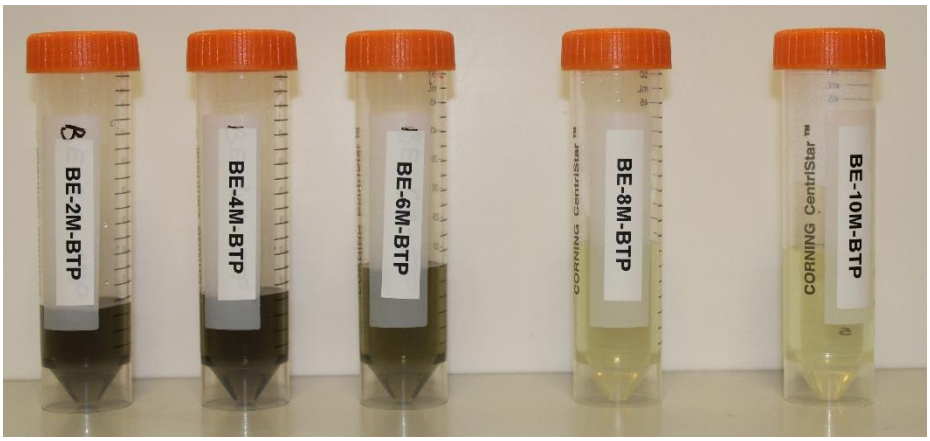

Figure 18: Photographs of final samples of 1 g/l s-BTP refluxed for ~20 hours (left to right) 2, 4, 6, 8, 10 mol/l nitric acid.

TOTAL ORGANIC CARBON MEASUREMENTS:S-BTP

The estimated carbon content of s-BTP can be (structurally) calculated as 49 wt%. For the 1 g/l s-BTP solutions, the carbon content can be expected to be *ca.* 0.49 g/l. From the total carbon results, the initial total carbon content of the samples is >1 g/l and increased with increasing reflux time, except those at high nitric acid concentrations, examples are shown in Figure 19. Concentration of the samples by evaporation does not explain this increase. These results suggest that the reagents were contaminated, possibly from organic components extracted from components in the apparatus (sampling tube). These results are of limited value and are not considered further.

This project has received funding from the EURATOM research and training programme 2014-2018 under grant agreement No 755171. The content of this deliverable reflects only the author's view. The European Commission is not responsible for any use that may be made of the information it contains.

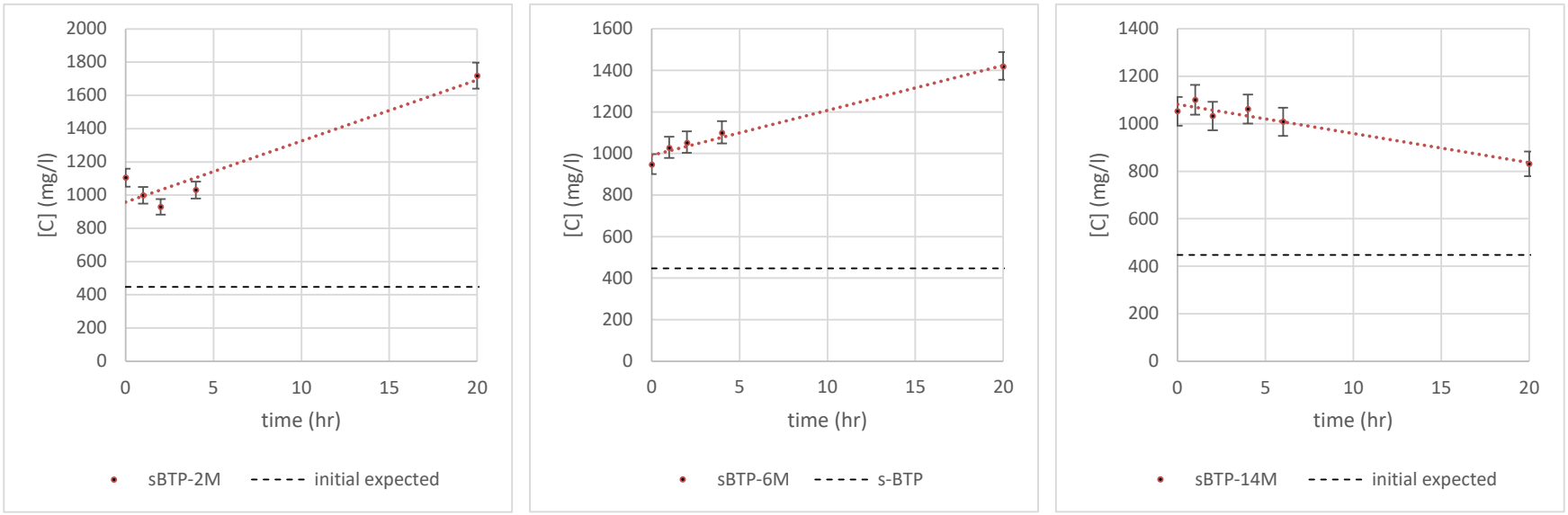

Figure 19: Total carbon content of 1 g/l s-BTP reflux at 2, 6 and 14 mol/l nitric acid

This project has received funding from the EURATOM research and training programme 2014-2018 under grant agreement No 755171. The content of this deliverable reflects only the author's view. The European Commission is not responsible for any use that may be made of the information it contains.

UV-VIS MATRIX METHOD MEASUREMENTS:– S-BTP

Inspection of the UV-Vis spectra of the s-BTP/iron(II) complex show a change in the shape of the spectra compared to the calibration curve, Figure 20. There is an initial increase in the absorbance of the main absorption bands at 471 nm and 578 nm over time, followed by a decrease in absorption. A loss of structure of the absorption bands at low acidity, e.g. 2 mol/l nitric Figure 20 (left), and to a lesser extent at higher acidity, e.g. 12 mol/l nitric acid Figure 20 (right) is accompanied by an appearance of a new absorption band centred around 720 nm. The new absorption band increases with time, apart from the 20 hour samples at high nitric acid concentrations, the peak disappears as the whole spectra flattens, suggesting that any complexing ability has been destroyed. These results indicate that there is a decrease in concentration of the s-BTP and any oxidation products with the ability to complex to iron(II). However, there is also an increase in an additional component, which can be assumed to be an s-BTP oxidation product. Although, the effect of the unknown organic contamination is also possible, similar effects were not observed with PTD, which are discussed the next section. On this basis, the appearance of a new band at 720 nm is consistent with a change in the s-BTP structure. The spectral shift to higher wavelengths is consistent with an increase in the strength of the complex, which may be indicative of nitration of the s-BTP ring structure, increasing electron withdrawing on the ring structure.

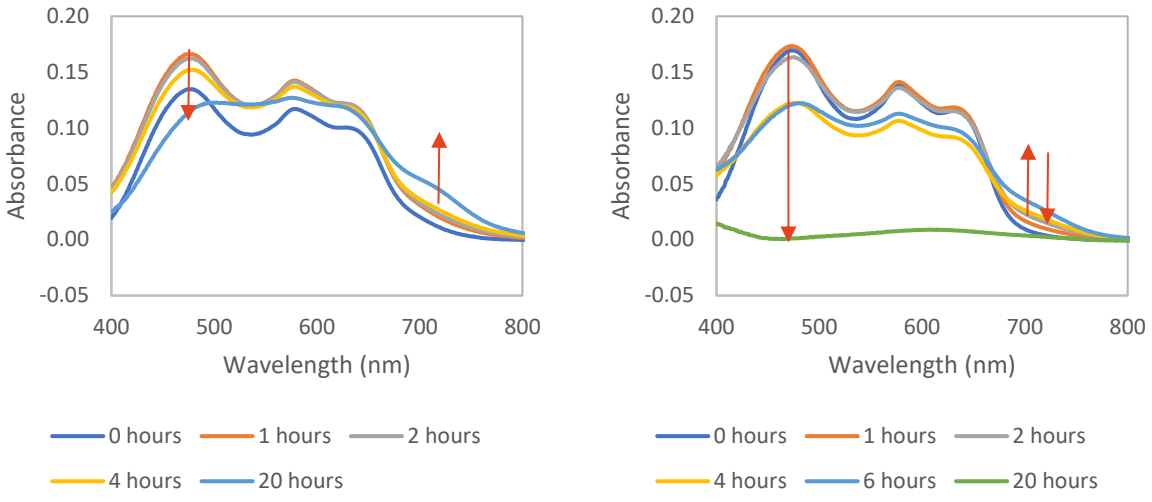

Figure 20: Baseline corrected absorbance spectra of Fe(II) complex of samples taken from reflux of 1 g/l s-BTP in 2 (left) and 12 (right) mol/l nitric acid

This project has received funding from the EURATOM research and training programme 2014-2018 under grant agreement No 755171. The content of this deliverable reflects only the author's view. The European Commission is not responsible for any use that may be made of the information it contains.

Despite the changes to the absorption spectra of the iron(II) complex, the concentration of s-BTP can be calibrated. It is recognised that these concentrations are approximate and are biased by the change in the absorption spectra, which can be assumed to be an s-BTP oxidation product that retains the ability to complex to iron(II). Examples of the s-BTP concentration over time are shown in Figure 21. A 1 g/l s-BTP sample is equivalent to 1.05 mmol/l s-BTP, however the determined concentrations have a variable initial concentration between 0.33-0.65 mmol/l s-BTP, Figure 22. At the '20 hour' sample there is no measurable s-BTP in 12 or 14 mol/l nitric acid. It is possible that the delay between the reflux experiments and iron(II) complex analysis could be a reasonable explanation for the decrease in initial concentrations, *i.e.* room temperature oxidation of s-BTP. Using this s-BTP data (except 0 hrs), with these uncertainties, natural log of concentration (Ln[s-BTP]) vs. time (hour) plots result in reasonably linear plots for limited data points. This suggests that the decomposition rate is proportional to the s-BTP concentration, suggesting a first order relationship. Plotting the calculated rate constants for each nitric acid concentration, Figure 23, shows a 2nd order dependence upon nitric acid concentration, $[HNO_3]^2$. These results suggest that the complexing component of s-BTP can be removed by reflux in moderate to high concentrations of nitric acid, whilst lower nitric acid concentrations suggest an increase the strength of the complex.

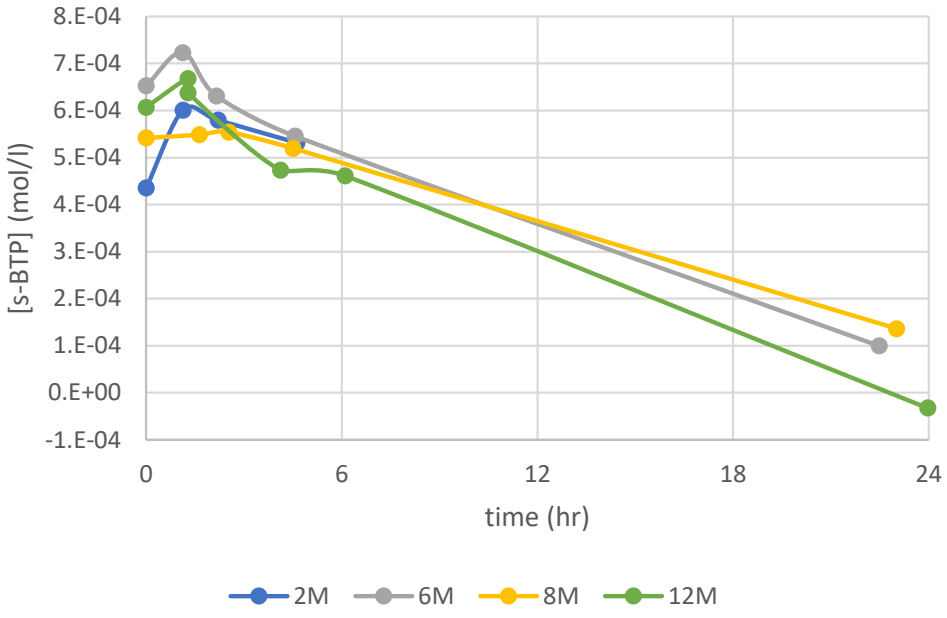

Figure 21: Concentration of s-BTP over time in nitric acid at reflux, concentration of nitric acid shown in legend.

This project has received funding from the EURATOM research and training programme 2014-2018 under grant agreement No 755171. The content of this deliverable reflects only the author's view. The European Commission is not responsible for any use that may be made of the information it contains.

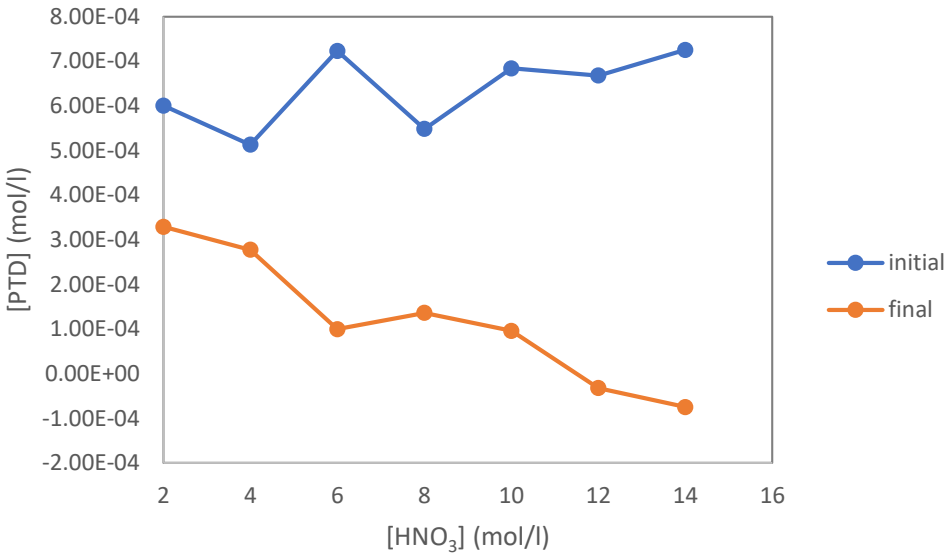

Figure 22: Effect of nitric acid concentration upon initial and final determined PTD concentration

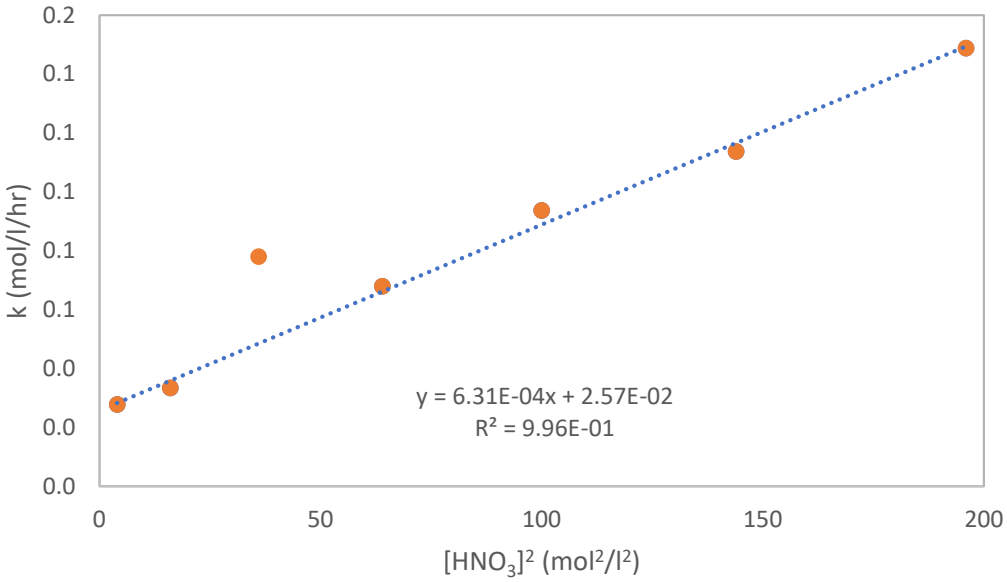

Figure 23: Effect of nitric acid concentration upon the rate of s-BTP oxidation

This project has received funding from the EURATOM research and training programme 2014-2018 under grant agreement No 755171. The content of this deliverable reflects only the author's view. The European Commission is not responsible for any use that may be made of the information it contains.

PTD DECOMPOSITION OF LIGANDS IN HOT NITRIC ACID

1 g/l PTD solutions are colourless, so no visual observations were made.

TOTAL ORGANIC CARBON RESULTS - PTD

The carbon content can be (structurally) calculated to be 55 wt%. As the solutions are 1 g/l PTD, solutions can be expected to be *ca.* 0.55 g/l C. In a similar manner to the results from s-BTP studies, the total organic carbon content is predominantly >1 g/l, shown in Figure 24 and amount of organic carbon increases over time, compared to an expectation of a decrease. As with the s-BTP, these results suggest carbon contamination and consequently the results are of limited value and are not considered further.

This project has received funding from the EURATOM research and training programme 2014-2018 under grant agreement No 755171. The content of this deliverable reflects only the author's view. The European Commission is not responsible for any use that may be made of the information it contains.

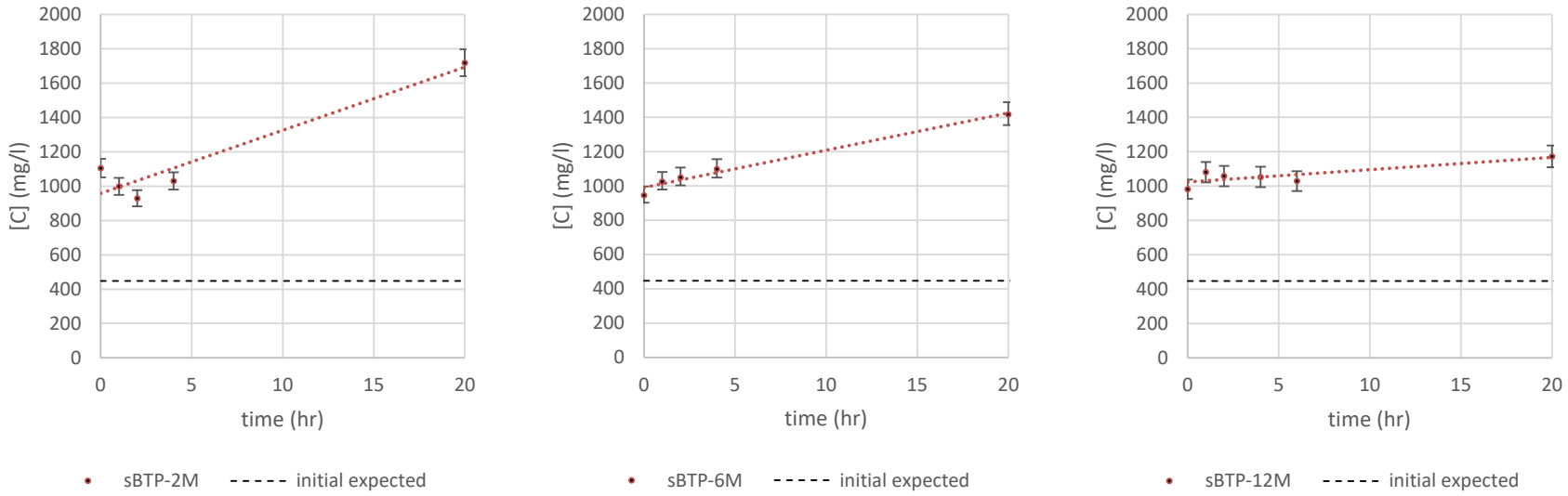

Figure 24: Total carbon content of 1 g/l PTD reflux at 2, 6 and 14 mol/l nitric acid

This project has received funding from the EURATOM research and training programme 2014-2018 under grant agreement No 755171. The content of this deliverable reflects only the author's view. The European Commission is not responsible for any use that may be made of the information it contains.

UV-VIS MATRIX METHOD MEASUREMENTS - PTD

Inspection of the UV-Vis absorption spectra of the iron(II) complex in hydroxylamine acetate buffer show a change in the spectra compared to the calibration curve, Figure 25. Similarly to the s-BTP, PTD at low acidity shows an increase in the observed iron(II) complex absorbance, whilst at higher nitric acid concentrations the observed PTD concentration reduces. Unlike the s-BTP, there are no substantial spectral changes. The apparent increase in PTD concentration at low acidity suggests that there is an increase in the apparent complex formation, which cannot be explained by evaporation.

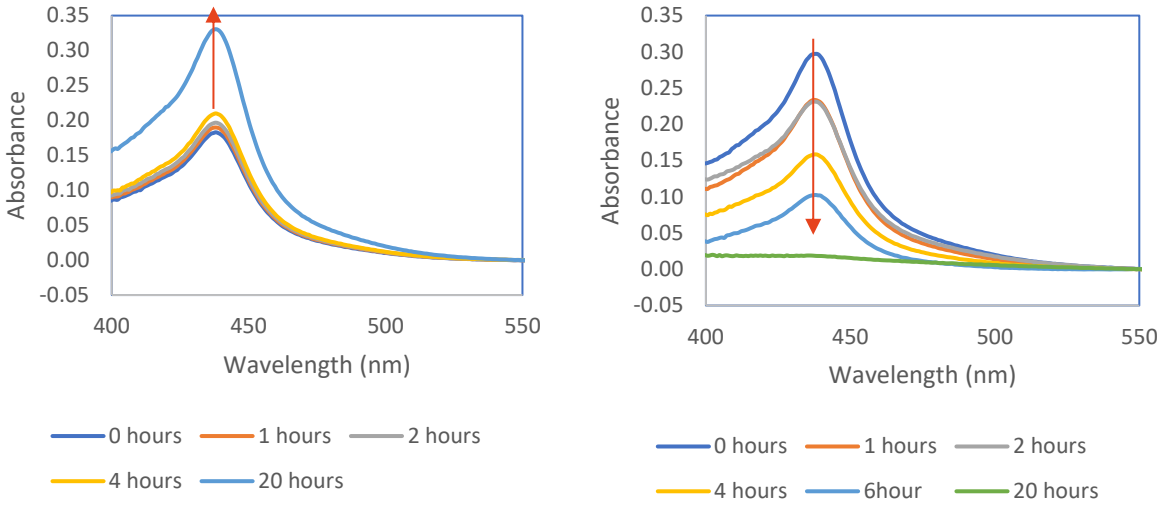

Figure 25: Baseline corrected absorbance spectra of Fe(II) complex of samples taken from reflux of 1 g/l PTD in 2 (left) and 12 (right) mol/l nitric acid

Similar to the s-BTP, as the apparent PTD concentration based on the iron(II) complex in a hydroxylamine acetate buffer increases at low nitric acid concentrations, it must be assumed that changes occur to the PTD to form a stronger complex. It is recognised that these results provide an indication of the complexing strength, but do not represent the actual PTD concentrations. Examples of the PTD concentration over time are shown in Figure 26. A 1 g/l PTD sample is equivalent to 3.04 mmol/l the as analysed initial results range from 3.3-6.3 mmol/l in 2-4 mol/l and >6 mol/l nitric acid being 5.4-6.3 mol/l, Figure 27. These results may suggest that changes are occurring at room temperature. Whilst the final, '20 hr' sample, has an apparent PTD concentration (or PTD with the ability to complex with iron(II)) reduced to near zero in >12 mol/l nitric acid. In a similar matter to s-BTP, plotting natural log of concentration (Ln[PTD]) vs. time (hour) plots resulted in reasonably linear plots for the limited data points (not shown). This suggests that the decomposition rate is proportional to

This project has received funding from the EURATOM research and training programme 2014-2018 under grant agreement No 755171. The content of this deliverable reflects only the author's view. The European Commission is not responsible for any use that may be made of the information it contains.

the PTD concentration, indicating a first order relationship. Plotting the calculated rate constants for each nitric acid concentration, Figure 28, shows a 2nd order dependence upon nitric acid concentration, $[HNO_3]^2$. These results suggest that the complexing component of PTD can be removed by reflux in moderate to high concentrations of nitric acid, whilst lower nitric acid concentrations suggest an increase in the strength of the complex.

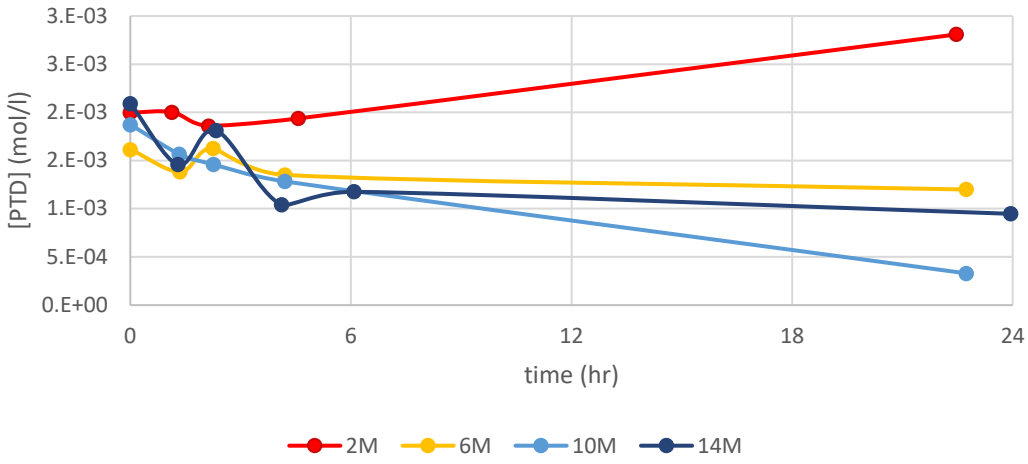

Figure 26: Concentration of PTD over time in nitric acid at reflux, concentration of nitric acid shown in legend

This project has received funding from the EURATOM research and training programme 2014-2018 under grant agreement No 755171. The content of this deliverable reflects only the author's view. The European Commission is not responsible for any use that may be made of the information it contains.

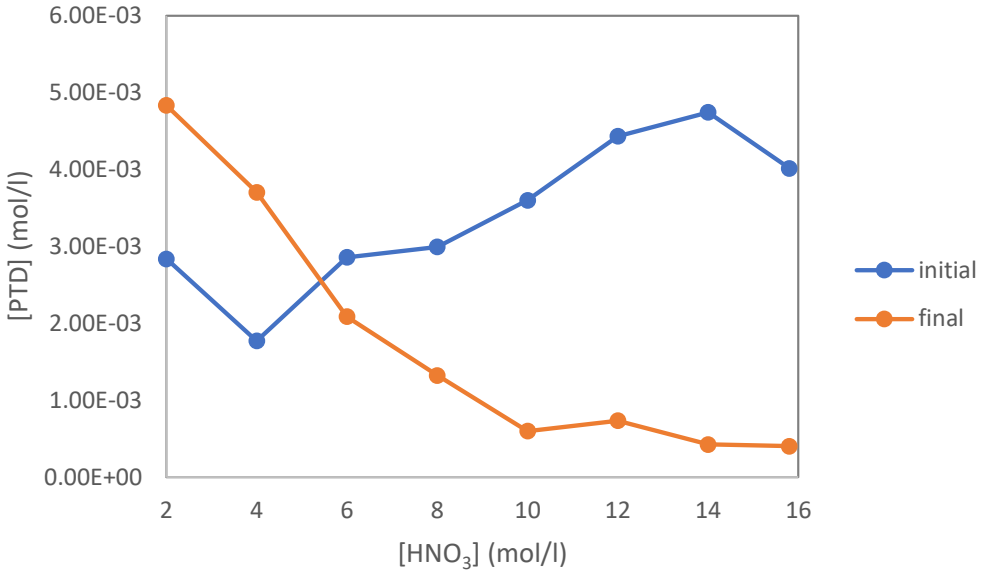

Figure 27: Effect of nitric acid concentration upon initial and final determined PTD concentration

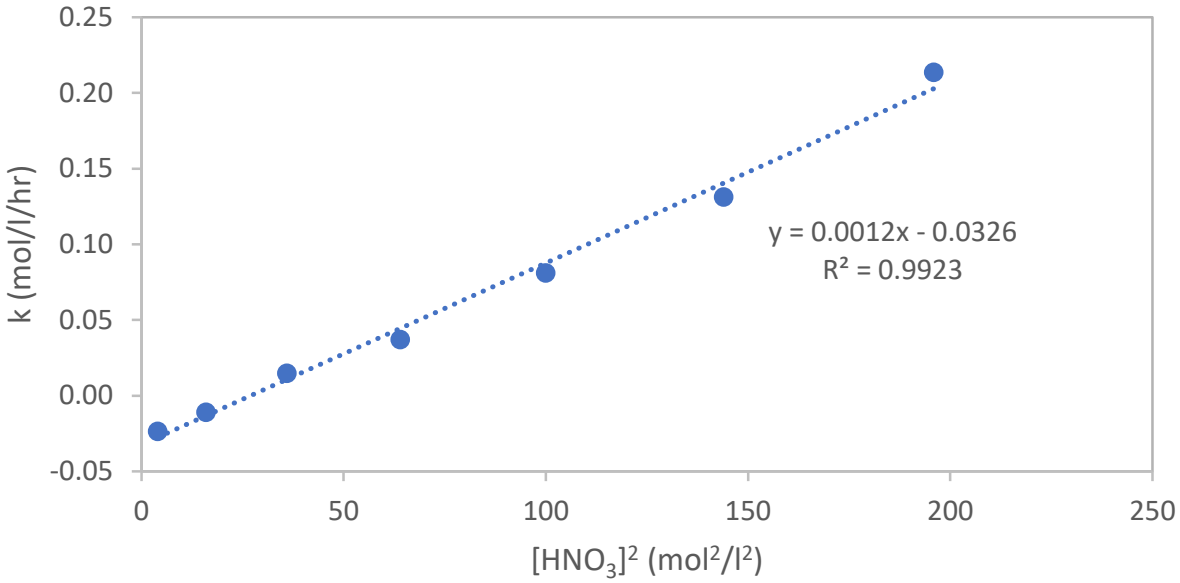

Figure 28: Effect of nitric acid concentration upon the rate of PTD oxidation

This project has received funding from the EURATOM research and training programme 2014-2018 under grant agreement No 755171. The content of this deliverable reflects only the author's view. The European Commission is not responsible for any use that may be made of the information it contains.

EFFECT OF HOT NITRIC ACID - SUMMARY

The refluxing of s-BTP and PTD in moderate to high concentrations of nitric acid for a period of 20-24 hours is sufficient to modify the structure of s-BTP and PTD such that no iron(II) complexation occurs. Work with americium has not been carried but it may be assumed that these results with iron(II) provide an indication of the strength of complexing ability to americium or other ions in solution. The refluxing of s-BTP and PTD at low nitric acid concentrations appears to show an increase in the complexing ability of the solutions, which may indicate structural changes are occurring that maintain their complexing ability. Given these preliminary experiments indicate refluxing in concentrated nitric acid HNO_3 is at least partially effective in destroying the ligands, the evaporation of solutions containing s-BTP and PTD is worthy of further investigation as an economic means of treatment prior to the return of OML to the separation process. In particular, further experiments to accurately quantify the decrease in carbon content in solution are needed. Interestingly, the rates of decomposition of both ligands appear to be proportional to $[HNO_3]^2$.

This project has received funding from the EURATOM research and training programme 2014-2018 under grant agreement No 755171. The content of this deliverable reflects only the author's view. The European Commission is not responsible for any use that may be made of the information it contains.

ELECTROCHEMICAL OXIDATION STUDIES OF PROCESS LIGANDS

Previous studies have shown that electrochemical oxidation can be used to oxidise soluble ligands without addition of a catalyst, whereas some ligands are more stable and require addition of a catalyst [14]. These processes are termed direct and mediated electrochemical oxidation (DEO and MEO) respectively. The addition of a catalyst generally increases oxidation rates. This work aims to carry out an initial study to assess the feasibility of oxidation using DEO and MEO with silver to oxidise PTD. DEO is preferrable as the process does not require the addition of a salt and could be applied before oxalate precipitation. Whilst, MEO where a salt is added, such as silver, would lead to contamination of the product, so is only applicable for application to the oxalate mother liquor (OML).

Earlier experiments where DEO and MEO have been applied, have used a flow electrolysis technique, which is readily translatable to industrial scale. The process technique uses a relatively large volume of working solutions (0.5-1.0 L) and uses a relatively large amount of equipment. Due to the low availability and high cost of PTD, this work aims to continue this work at small scale with dilute PTD solutions. As s-BTP is available in the laboratory and is currently not in high demand, initial proving experiments using s-BTP allowed methods to be tested before the PTD experiments were carried out.

Boron doped diamond (Nb/BDD) electrodes have been used for DEO studies, due to the high oxygen over-potential, compared to other electrodes that can be used in nitric acid at high potentials, such as platinum or platinised titanium (Ti/Pt). To effectively use BDD electrodes for DEO it is advantageous to have effective agitation. It is also known that the use of BDD as stationary electrode can lead to delamination of the BDD coating [55]. As the studies aim to oxidise the ligand the electrode surface area must be sufficient to allow enough charge (Q = It) to be passed in a reasonable time (working day) to allow oxidation of the amount of ligand under study. For these reasons, the use of a large rotating disc electrode (RDE) therefore fills these requirements. RDE have the advantage that their defined hydrodynamic conditions are more likely to be related to flow electrolysis cells, which in turn can be related to industrial scale cells.

To assess the oxidation of the ligands two types of studies have been carried out:

- Cyclic voltammetry (CV) – as a quick method that may provide an initial indication of whether the ligands can be oxidised or reduced.
- Electrolysis on a rotating disc – aimed at oxidising the ligand with and without a silver catalyst (MEO and DEO respectively). The residues from these experiments will then be oxidised by silver(II) by electrolysis in a beaker electrochemical cell.

This project has received funding from the EURATOM research and training programme 2014-2018 under grant agreement No 755171. The content of this deliverable reflects only the author's view. The European Commission is not responsible for any use that may be made of the information it contains.

CYCLIC VOLTAMETRY

EXPERIMENTAL

To assess the stability of s-BTP and PTD towards oxidation and reduction, cyclic voltammetry was a good starting point to assess whether there are any rapid oxidation or reduction reactions. These experiments used a small beaker volumetry cell (ALS VC-4) with 1.6 mm∅ platinum voltammetry electrode (ALS PTE). A platinum wire counter electrode was separated from the working electrode using a glass tube with glass frit. Reference electrode measurements were made using a gelled Ag/AgCl reference electrode (Sentek R2/AGCL/KNO3/GEL/1M/4MM, *ca.* 0.20 V_{NHE}) connected to the voltammetry cell using a salt bridge, made using 1/16" PVDF tube lined with glass wool strands. Cyclic voltammograms were made using a IviumStat.h potentiostat. The cell used is shown in Figure 29.

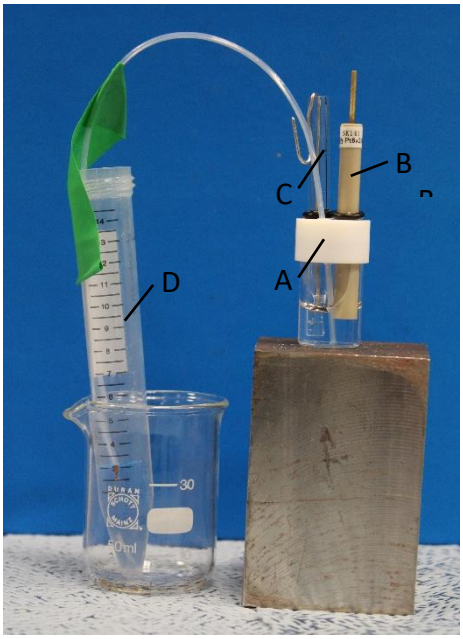

A – voltammetry cell, B – Pt working electrode, C – Counter electrode in separate compartment, D – Reference electrode measurement compartment with salt bridge (reference electrode not shown)

Figure 29: Voltammetry cell

This project has received funding from the EURATOM research and training programme 2014-2018 under grant agreement No 755171. The content of this deliverable reflects only the author's view. The European Commission is not responsible for any use that may be made of the information it contains.

RESULTS

A series of CVs with and without 1 g/l s-BTP (Mr 949.8 g/mol, 1 mmol/l) or PTD (Mr 326.3 g/mol, 3 mmol/l) in 1 mol/l nitric acid medium with 16 mol/l nitric acid as a counter electrode medium over a range of scan rates, 10-250 mV/s were recorded. Figure 30 compares the oxidation (0.8 to 2 $V_{Ag/AgCl}$) of 1 g/l s-BTP and PTD with the matrix 1 mol/l nitric acid. These curves show an increase in current at >1.6 $V_{Ag/AgCl}$, consistent with the oxidation of water. There was no pronounced enhancement of current with the addition of PTD and s-BTP present, that could be attributed to oxidation of the ligand. This could be due to the low ligand concentration.

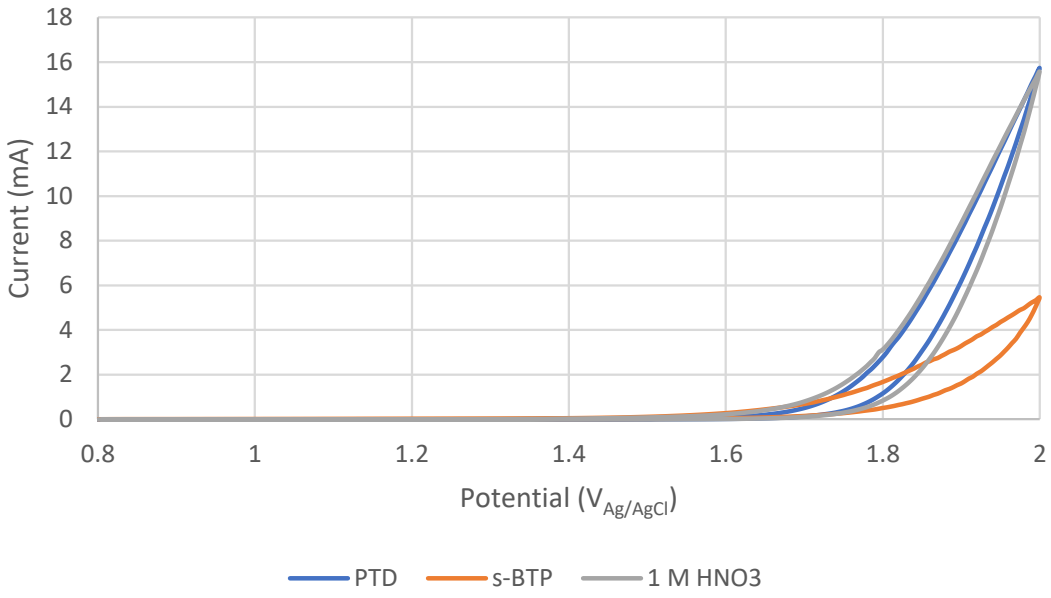

Figure 30: Oxidation cyclic voltammogram 0.8-2 $V_{Ag/AgCl}$, 250 mV/s, 1 mol/l nitric acid with and without 1 g/l s-BTP or PTD.

This project has received funding from the EURATOM research and training programme 2014-2018 under grant agreement No 755171. The content of this deliverable reflects only the author's view. The European Commission is not responsible for any use that may be made of the information it contains.

Although not the focus of this work, the reduction CVs where also recorded as it was not a large amount of additional work and it is relevant to flowsheet development. The addition of a reduction process could be used as part of the finishing process in the co-finishing of uranium with plutonium and/or minor actinides, where reduction could change the behaviour of the ligand. Figure 31 compares the reduction (0.8 to 0 $V_{Ag/AgCl}$) of 1 g/l s-BTP and PTD with the matrix 1 mol/l nitric acid. The reduction peaks at *ca.* 0.2 $V_{Ag/AgCl}$ correspond to the hydrogen adsorption upon the platinum electrode. There is no distinct reduction of PTD. s-BTP shows an additional peak at *ca.* 0.1 $V_{Ag/AgCl}$, which may be due to s-BTP reduction or change to Pt hydrogen absorption. Work at higher concentrations of s-BTP and PTD is needed to provide conclusive results.

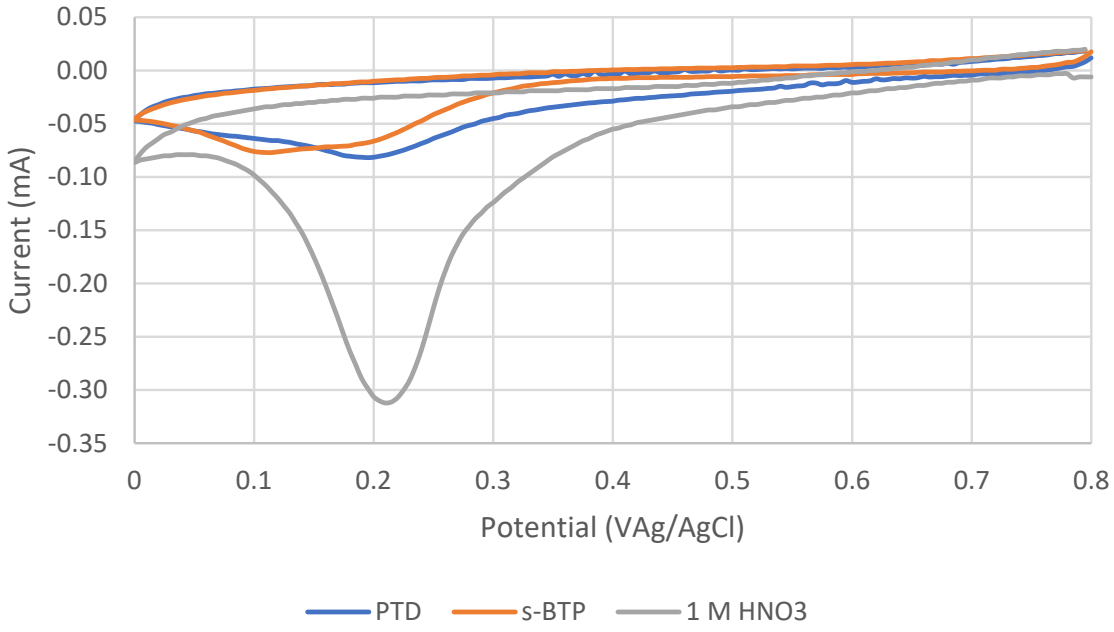

Figure 31: Reduction cyclic voltammogram 0.8-0 $V_{Ag/AgCl}$, 250 mV/s, 1 mol/l nitric acid with and without 1 g/l s-BTP or PTD.

This project has received funding from the EURATOM research and training programme 2014-2018 under grant agreement No 755171. The content of this deliverable reflects only the author's view. The European Commission is not responsible for any use that may be made of the information it contains.

ELECTROCHEMICAL OXIDATION

EXPERIMENTAL

ROTATING DISC EQUIPMENT

A key first step to this work was the identification of suitable equipment. A commercially available RDE was selected for these studies; the OrigaTrod produced by Origalys, France (supplied by Alvatek Ltd, UK) system. The OrigaTrod key features are:

- BDD electrode in the standard catalogue with chemical resistant housing (PEEK),
- can be used at high currents (upto 1 A),
- can be readily incorporated into glassware (has standard glass taper on motor housing),
- manufacturer sells glassware that can be used with the equipment.

The OrigaTrod includes a taco-controlled motor in a housing with control box, software control and a removable interchangeable tip. A tip includes a sample holder and 18 mm∅ × 3 mm depth BDD coated pellet. The electrode with holder fits inside the OrigaCell, which consists of a glass beaker and five 14/23 port lid with simple glass flange. The OrigaCell lid assembled to include:

- separate counter electrode compartment (OrigaSens salt bridge junction) containing a 1.6 mm∅ titanium wire to form the cathode. This compartment included an air purge and water-cooled condenser,
- PTFE coated K-type thermocouple,
- purge inlet,
- Purge outlet via water cooled condenser,
- 3.2 mm∅ tube for sampling solution,
- Salt bridge made from a 1.6 mm∅ PVDF tube containing glass wool. The salt bridge connected to a separate tube containing a gelled double junction Ag/AgCl electrode (Sentek R2/AGCL/KNO3/GEL/1M/4MM).

The anode and cathode compartments were air purged to minimise the accumulation of potentially flammable gas mixtures. Initially condensers were connected to gas wash bottles; however, these were later removed as the OrigaCell simple glass flange could not be sealed when a gas purge was applied. This resulted in the generation of a higher pressure in the counter electrode compartment (which was sealed) and the counter electrode solution was

This project has received funding from the EURATOM research and training programme 2014-2018 under grant agreement No 755171. The content of this deliverable reflects only the author's view. The European Commission is not responsible for any use that may be made of the information it contains.

forced into the working solution. All later experiments the gas wash bottles were removed. The assembled apparatus is shown in Figure 32.

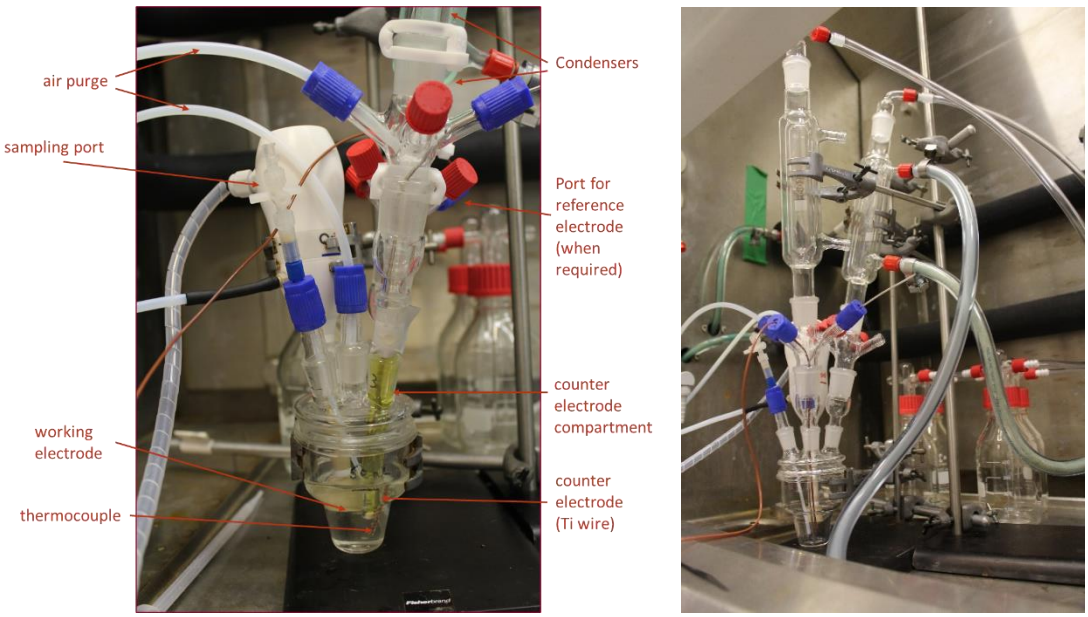

Figure 32: Electrolysis cell including BDD rotating disc electrode

RDE – SELECTION OF CONDITIONS FOR OXIDATION

Initially experiments aimed for familiarisation with the equipment and selection of conditions for later experiments. These were carried out by completing two series of linear sweep voltammetry experiments using a IviumStat.h potentiostat under the conditions listed in Table 6.

This project has received funding from the EURATOM research and training programme 2014-2018 under grant agreement No 755171. The content of this deliverable reflects only the author's view. The European Commission is not responsible for any use that may be made of the information it contains.

Table 6: RDE linear sweep voltammetry conditions

Series	Working solution (50 ml)	Linear voltammetry conditions	Catholyte solution (9 ml)
1	0.1 mol/l $AgNO_3$ – 6 mol/l nitric acid	1.5-2.0 $V_{Ag/AgCl}$ 250-10 mV/s and 0-5000 rpm	16 mol/l nitric acid
2	0-0.2 mol/l $AgNO_3$ – 6 mol/l nitric acid	1.5-2.0 $V_{Ag/AgCl}$ 10 mV/s 3000 rpm	16 mol/l nitric acid
	0.1 mol/l $AgNO_3$ – 6 mol/l nitric acid	1.5-2.5 $V_{Ag/AgCl}$ 10 mV/s 3000 rpm	16 mol/l nitric acid

OXIDATION OF S-BTP AND PTD – BULK ELECTROLYSIS RDE STUDIES

To assess the oxidation of s-BTP and PTD by DEO and silver MEO four experiments were carried out at 1 g/l s-BTP or PTD:

- 0.5 ml of 100 g/l s-BTP added to 50 ml 0.1 mol/l $AgNO_3$ in 6 mol/l HNO_3,
- 0.5 ml of 100 g/l s-BTP added to 50 ml 6 mol/l HNO_3 in the RDE cell,
- 0.5 ml of 100 g/l PTD added to 50 ml 6 mol/l HNO_3 in the RDE cell,
- 0.5 ml of PTD added to 50 ml 0.1 mol/litre $AgNO_3$ in 6 mol/l HNO_3 in the RDE cell.

Each solution was mixed using rotation of the RDE, and a zero-hour sample taken. A DC power supply, PSU (model TTi EL30) was set to a constant current of 0.1 A. Samples were taken at 0, 0.5, 1, 2, 3, 4, 5 and 6 hour time points. The time point samples were run on the UV-Vis using the s-BTP matrix method, with a modification of filtration to remove the silver chloride precipitate formed if $AgNO_3$ was present. For the PTD samples, the samples were allowed >30 mins complexation time before analysing. The samples were photographed once the Ag(II) had decomposed. 1 ml of each timepoint sample for each experiment was tenfold diluted and sent for total carbon analysis (Shimadzu TOC-L).The conditions of the experiments are listed in Table 7.

This project has received funding from the EURATOM research and training programme 2014-2018 under grant agreement No 755171. The content of this deliverable reflects only the author's view. The European Commission is not responsible for any use that may be made of the information it contains.

Table 7: Electrolysis conditions

Experiment	Electrolysis conditions	Working solution (50 ml)	
		[$AgNO_3$] (mol/l)	Ligand (1 g/l)
1	0.1 A at 2000 rpm	0	s-BTP
2	0.1 A at 2000 rpm	0.1	s-BTP
3	0.1 A at 2000 rpm	0	PTD
4	0.1 A at 2000 rpm	0.1	PTD

OXIDATION OF S-BTP AND PTD – BULK ELECTROLYSIS IN BEAKER

To carry out a practical demonstration of the oxidation of s-BTP and PTD a beaker electrolysis cell was used to assess the feasibility of removal of s-BTP and PTD from laboratory wastes prior to onward treatment. An electrolysis cell with large anode to volume ratio was set up as shown in Figure 33. This electrolysis cell is over engineered for these tests but it gave a useful demonstration of capabilities. This cell included:

- Four part custom glassware, with jacketed beaker, lid, cathode compartment with P4 glass frit and lid adapter,
- Ti/Pt mesh basket anode, Ti mesh basket cathode,
- Air purge to anode and cathode compartments,
- Thermocouple to allow measurement of anode compartment temperature,
- Anode compartment 3.2 mm∅ PVDF tube for sampling with syringe.

This project has received funding from the EURATOM research and training programme 2014-2018 under grant agreement No 755171. The content of this deliverable reflects only the author's view. The European Commission is not responsible for any use that may be made of the information it contains.

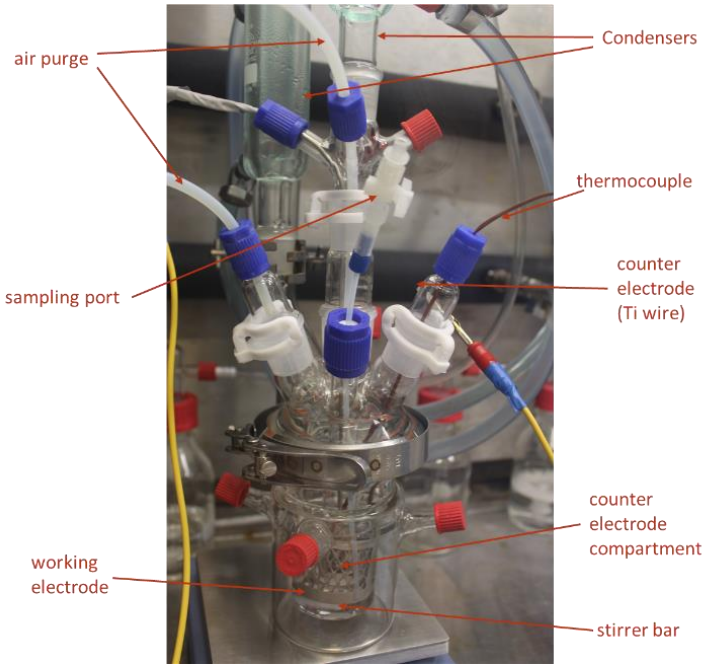

Figure 33 : Bulk electrolysis beaker cell

Residue from the previous s-BTP with $AgNO_3$ experiments was added to the bulk cell containing 50 ml 6 mol/l HNO_3. Ag(II) was generated, (shown by the visible colour change of the electrolyte) and the residue from the non-silver containing s-BTP experiments was added (~25 ml). A zero-hour sample was taken, and the cell run at 2.04 A for 45 mins with sampling. After completion of the s-BTP oxidation, 1 ml of 100 g/l PTD solution was added to the electrolyte. This was then run at 2.04 A for 45 minutes with sampling.

This project has received funding from the EURATOM research and training programme 2014-2018 under grant agreement No 755171. The content of this deliverable reflects only the author's view. The European Commission is not responsible for any use that may be made of the information it contains.

RESULTS

RDE – SELECTION OF CONDITIONS FOR OXIDATION

Electrolytes with a range of $AgNO_3$ concentrations between 0.01 and 0.2 mol/l were run in the RDE cell, over a potential sweep of 1.5-2 V. As shown Figure 34, as the rotation speed increases, the current recorded at 2 V is greater. The tests show an increase in current with rotation speed, Figure 35 and an increase in current with [$AgNO_3$], Figure 34 and Figure 35. At rotations >3000 rpm, the electrolyte showed increased turbulence and turbidity due to entrained air bubbles. This resulted in a greater number of splashes and increased likelihood of bubbles trapped under the electrode causing fluctuation in current generation. As a balance 2000 rpm was selected as the rotation speed to perform the oxidation of s-BTP and PTD experiments. A linear sweep between 1.5-2.5 $V_{Ag/AgCl}$ shows current of ~0.1 A at 2.5 $V_{Ag/AgCl}$, Figure 36.

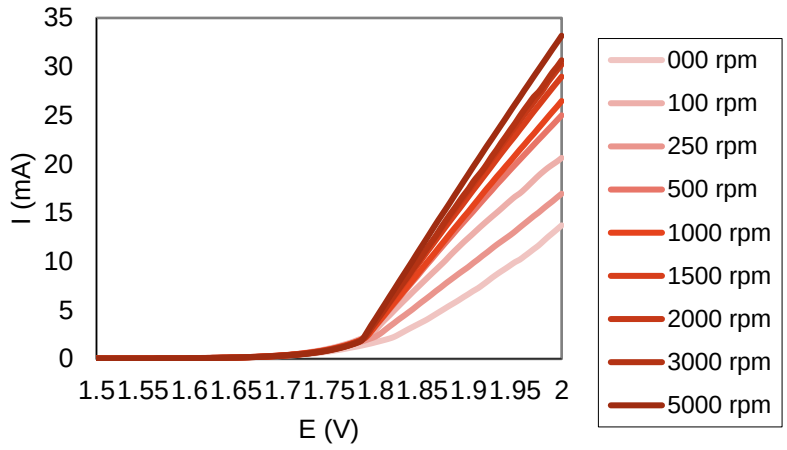

Figure 34: Linear sweep voltamograph, 1.5-2.0 $V_{Ag/AgCl}$,10 mV/s – generation of silver(II) - effect of rotation speed, 0-5000 /s, 6mol/l nitric acid – 0.1 mol/l $AgNO_3$. Legend: rotation rate (rpm) of RDE.

This project has received funding from the EURATOM research and training programme 2014-2018 under grant agreement No 755171. The content of this deliverable reflects only the author's view. The European Commission is not responsible for any use that may be made of the information it contains.

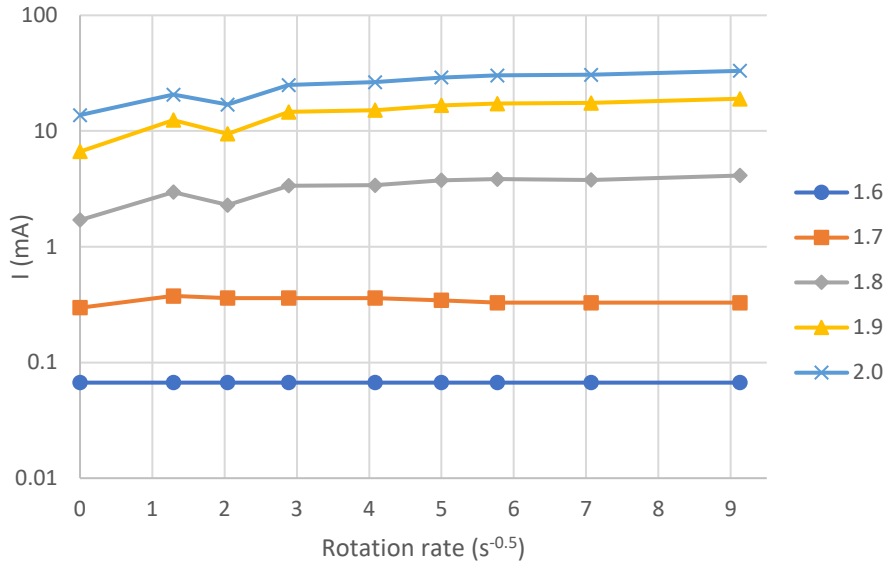

Figure 35: Effect of rotation rate upon current for different potentials

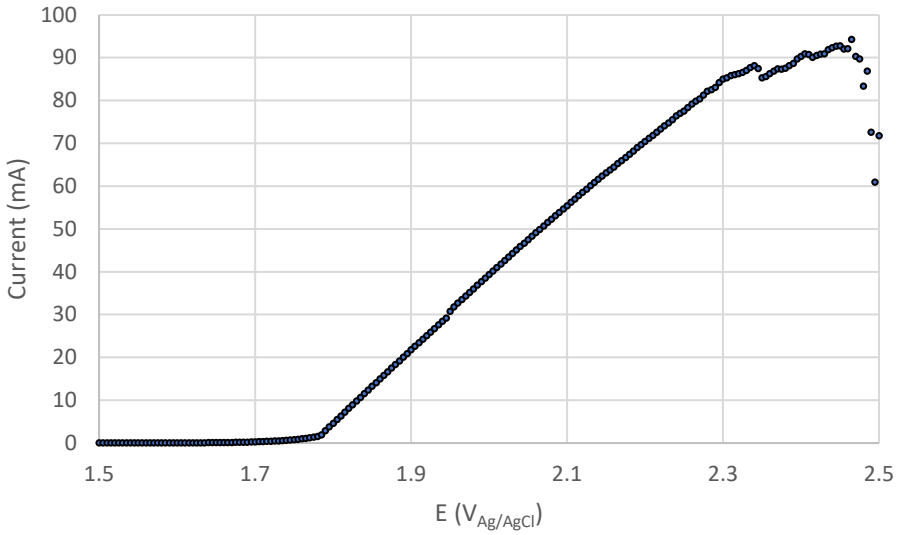

Figure 36: Linear sweep voltamograph, 1.5-2.5 VAg/AgCl 10 mV/s – generation of silver(II) - 3000 /min, 6 mol/l nitric acid – 0.1 mol/l AgNO3.

This project has received funding from the EURATOM research and training programme 2014-2018 under grant agreement No 755171. The content of this deliverable reflects only the author's view. The European Commission is not responsible for any use that may be made of the information it contains.

OXIDATION OF S-BTP AND PTD – BULK ELECTROLYSIS RDE STUDIES

The following results compare the oxidation of 1 g/l s-BTP at 0.1 A on a Nb/BDD electrode at 2000 rpm in 6 mol/l nitric acid and 0.1 mol/l $AgNO_3$ – 6 mol/l nitric acid. Initial samples of s-BTP are a yellow colour, the DEO samples remain coloured, whilst the MEO(Ag) quickly loses their colour, Figure 37. MEO(Ag) shows a more rapid reduction in complexant concentration (Figure 38) and total carbon content (Figure 39) compared to without silver (DEO). Removal of the complexant concentration with silver required *ca.* 0.5 hr compared with estimated 7 hours DEO. MEO(Ag) is 14 times faster than DEO at removing the complexing ability of the solution. The total carbon content of the solution is greater than 1 g/l, suggesting contamination of the solutions had occurred in a similar manner to the boiling tests. The total carbon oxidation with MEO(Ag) required *ca.* 4 hours compared to *ca.* 25 % reduction in 6 hours for DEO, or MEO(Ag) is approximately 7 times faster at total carbon removal. It should be noted that with the MEO(Ag) total carbon some residue carbon beyond 5 hours is above the total carbon LOD estimate of 0.002 g/l; however, the results are consistent with the organic contamination observed in the boiling tests. Quantification of the electrochemical efficiency of the process is made difficult by the presence of other unknown organic compounds. However, based on Eq 21, 2.8 hours can be estimated as the oxidation time at 100 % faradaic efficiency. MEO(Ag) and DEO oxidation proceeds at 65 and 9 % faradaic efficiency respectively, neglecting the effect of the additional carbon, which has not slowed the oxidation down to a great extent.

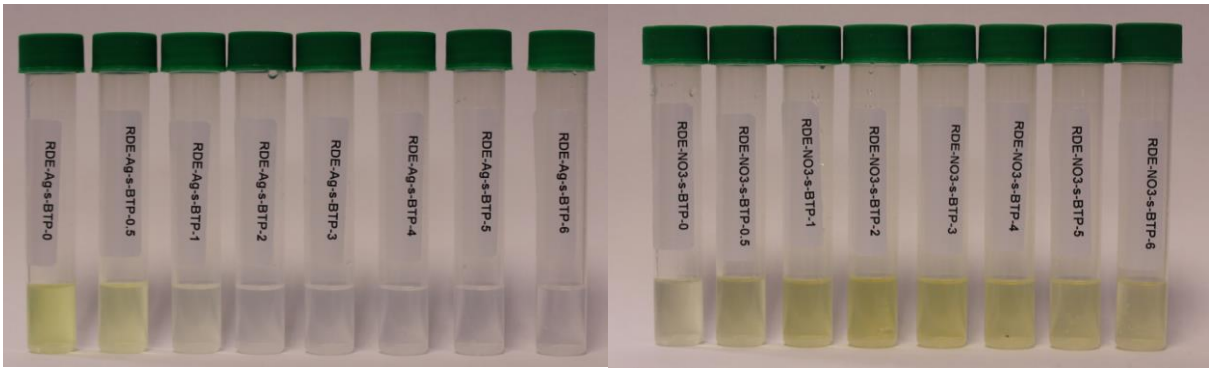

Figure 37: Colormetric change over time from RDE experiments: s-BTP with (left) and without (right) silver nitrate.

This project has received funding from the EURATOM research and training programme 2014-2018 under grant agreement No 755171. The content of this deliverable reflects only the author's view. The European Commission is not responsible for any use that may be made of the information it contains.

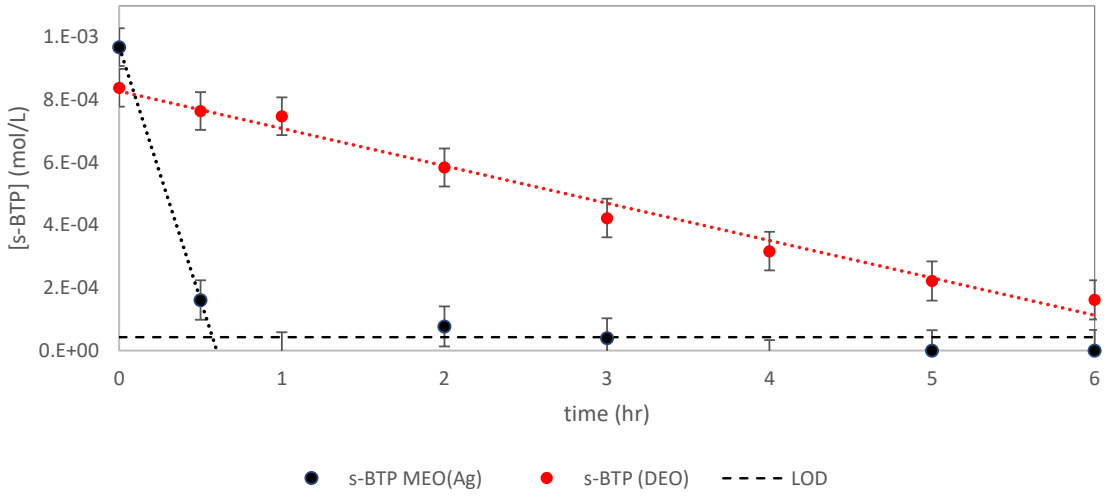

Figure 38: Electrochemical oxidation of s-BTP on BDD RDE DEO and MEO (Ag) – UV-Vis s-BTP concentration

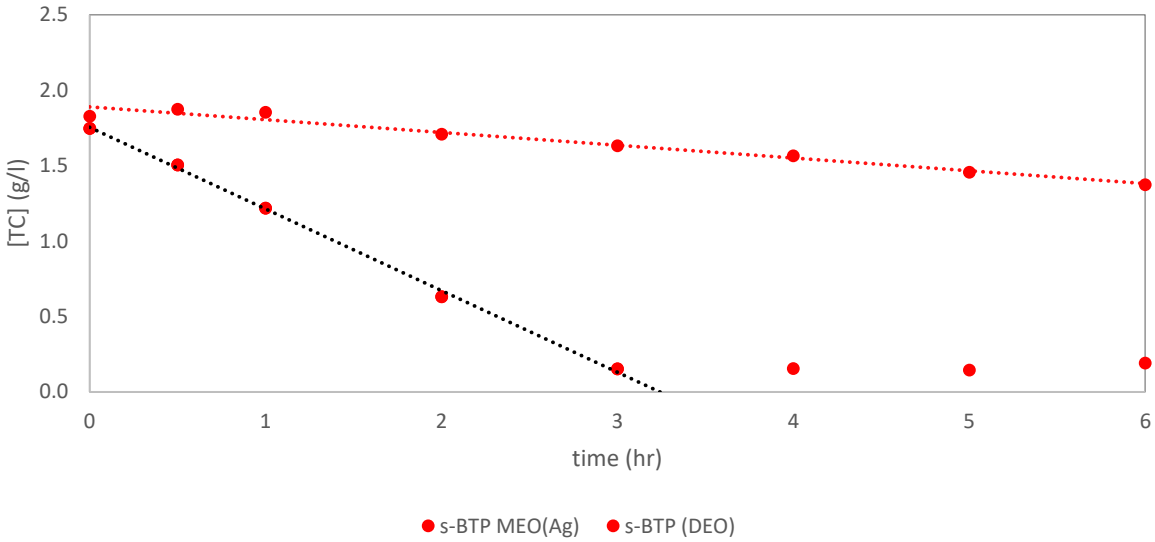

Figure 39: Electrochemical oxidation of s-BTP on BDD RDE DEO and MEO (Ag) – total carbon

$$C_{35}N_7H_{18}S_4O_{12}Na_4 + 95H_2O \rightarrow 35CO_2 + 7HNO_3 + 4HNaSO_4 + 198H^+ + 198e^- \quad \text{Eq 21}$$

This project has received funding from the EURATOM research and training programme 2014-2018 under grant agreement No 755171. The content of this deliverable reflects only the author's view. The European Commission is not responsible for any use that may be made of the information it contains.

The following results compare the oxidation of 1 g/l PTD at 0.1 A on a Nb/BDD electrode at 2000 rpm in 6 mol/l nitric acid and 0.1 mol/l $AgNO_3$ – 6 mol/l nitric acid. MEO(Ag) shows a more rapid reduction in complexant concentration (Figure 40) and total carbon content (Figure 41) compared to without silver (DEO). Based on the UV-Vis complexant concentration determination, MEO(Ag) substantially reduces the concentration within 1 hour. Based on the UV-Vis complexant determination, DEO reduces the concentration in *ca.* 5 hours. The total carbon content reduces more quickly in the presence of silver catalysis, MEO(Ag), compared to without, DEO. The total carbon content for PTD reduces to a lesser extent compared to s-BTP suggesting that PTD oxidation products are more stable compared to s-BTP oxidation products. PTD has a carbon content of 55 %, so oxidation based on Eq 22 should require *ca.* 4.5 hours, but as substantial carbon is present at the end of the 6 hour experiment, it is clear that the overall current efficiency is much less than 50 %.

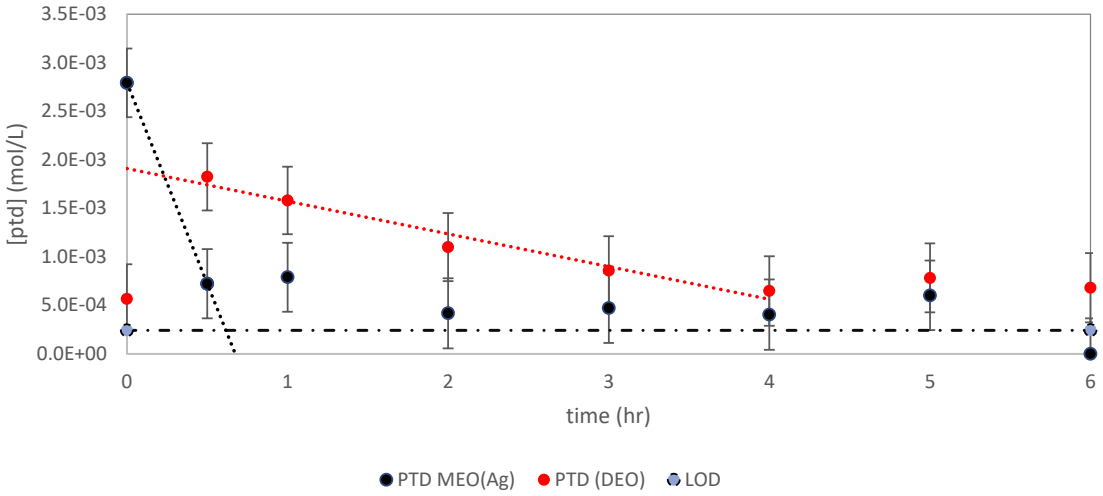

Figure 40: Electrochemical oxidation of PTD on BDD RDE DEO and MEO (Ag) – UV-Vis PTD concentration

This project has received funding from the EURATOM research and training programme 2014-2018 under grant agreement No 755171. The content of this deliverable reflects only the author's view. The European Commission is not responsible for any use that may be made of the information it contains.

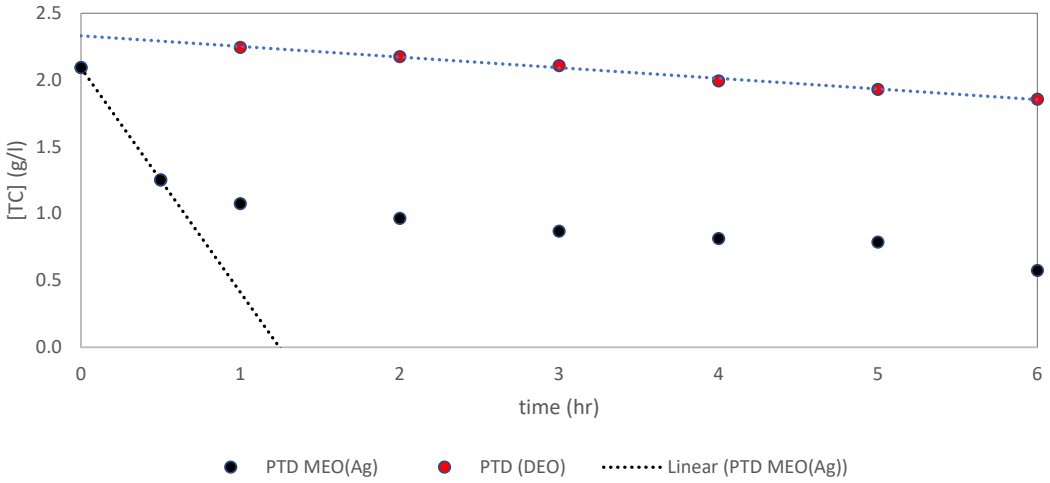

Figure 41: Electrochemical oxidation of PTD on BDD RDE DEO and MEO (Ag) – total carbon

$$C_{15}H_{19}N_7O_2 + 49H_2O \rightarrow 15CO_2 + 7HNO_3 + 110H^+ + 110e^- \quad \text{Eq 22}$$

This project has received funding from the EURATOM research and training programme 2014-2018 under grant agreement No 755171. The content of this deliverable reflects only the author's view. The European Commission is not responsible for any use that may be made of the information it contains.

OXIDATION OF S-BTP AND PTD – BULK ELECTROLYSIS IN BEAKER

The following studies aimed to compare the DEO and MEO oxidation rate of s-BTP and PTD, with two applied tests to oxidise s-BTP and PTD in a beaker electrolysis cell with silver(II) that are described here. The small amounts of s-BTP present in the residues from the RDE s-BTP studies were added to the beaker electrolysis cell and oxidised with silver, MEO(Ag). These results show a decline in the solution complexing ability as determined by the UV-Vis method (Figure 42) and total carbon (Figure 43). The oxidation of PTD shows similar results, by the UV-Vis method (Figure 44) and total carbon (Figure 45). The total carbon residues show higher than expected final carbon contents, but consistent with other results in this series. These tests show that s-BTP and PTD can be oxidised in laboratory wastes with silver(II).

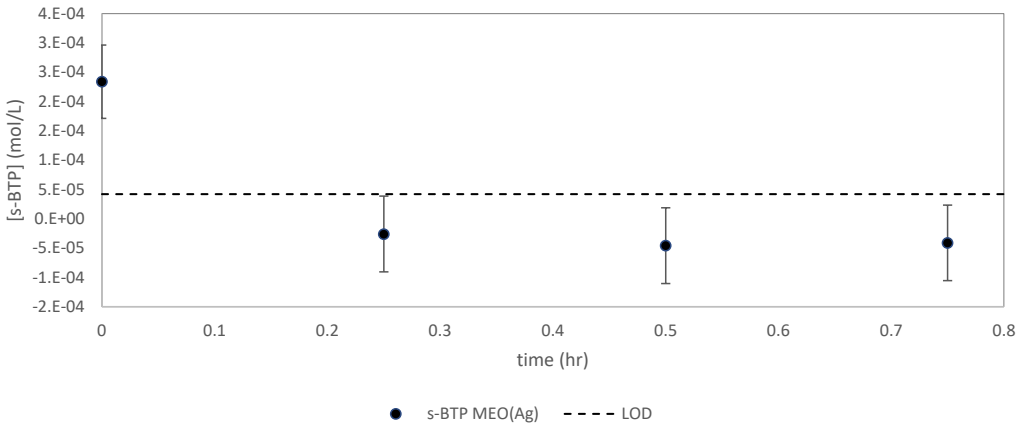

Figure 42: Electrochemical oxidation of s-BTP with beaker electrolysis cell DEO and MEO (Ag) – UV-Vis s-BTP concentration over time

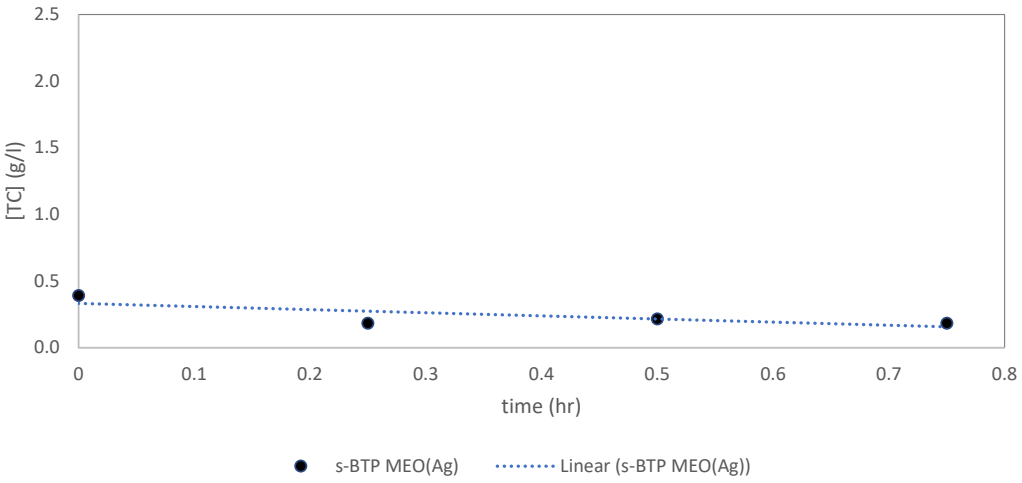

This project has received funding from the EURATOM research and training programme 2014-2018 under grant agreement No 755171. The content of this deliverable reflects only the author's view. The European Commission is not responsible for any use that may be made of the information it contains.

Figure 43: Electrochemical oxidation of s-BTP with beaker electrolysis cell DEO and MEO (Ag) – total carbon

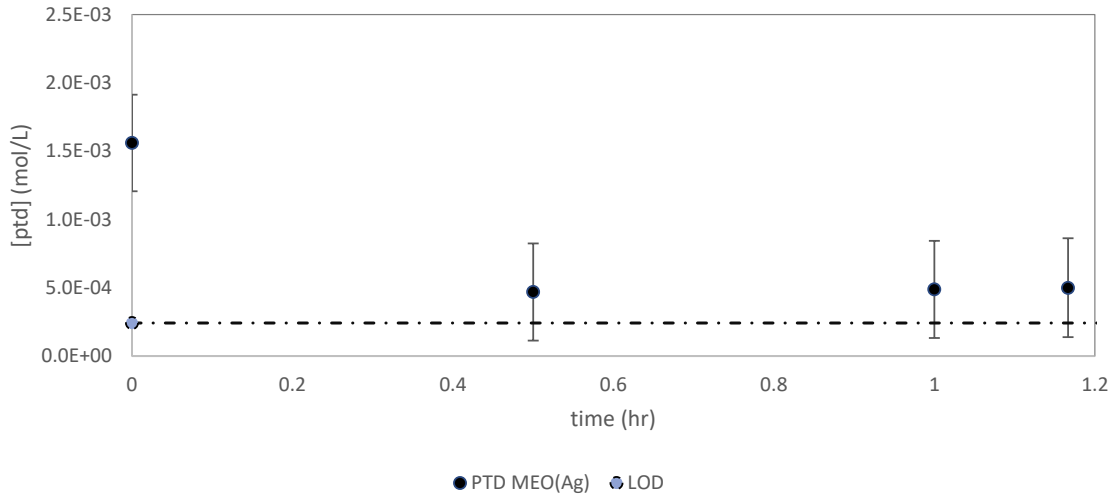

Figure 44: Electrochemical oxidation of PTD with beaker electrolysis cell DEO and MEO(Ag) – UV-Vis PTD concentration over time

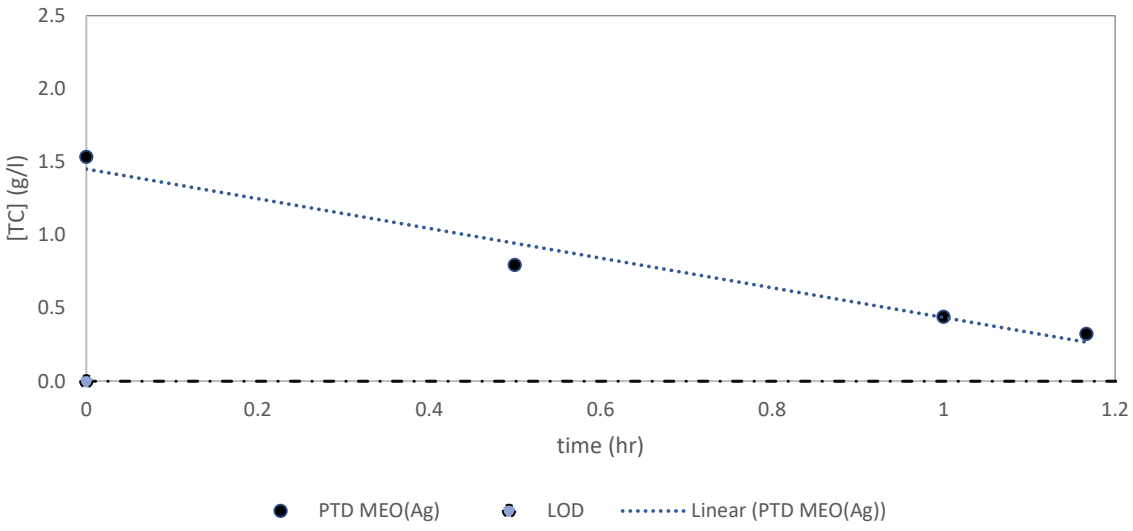

Figure 45: Electrochemical oxidation of PTD with beaker electrolysis cell DEO and MEO (Ag) – total carbon

This project has received funding from the EURATOM research and training programme 2014-2018 under grant agreement No 755171. The content of this deliverable reflects only the author's view. The European Commission is not responsible for any use that may be made of the information it contains.

ELECTROCHEMICAL OXIDATION SUMMARY

Electrochemical oxidation of s-BTP and PTD has been studied by using a rotating disc Nb/BDD electrode without silver (DEO) and with silver (MEO). These results show that there is a rapid removal of the complexing component in s-BTP and PTD by MEO. DEO has been shown to remove the complexing component at a rate 1 order of magnitude slower. These findings are similar to other complexant electrochemical oxidation studies where MEO is much faster than DEO. The results suggest that removal of s-BTP total carbon content is much faster compared to PTD, which indicates that PTD could have an oxidation product that is more stable towards oxidation. However, due to contamination of the samples with other organics, it is not possible to make definitive conclusions about the removal of remaining component of the ligands, other than there is a decline in the carbon content. Based on earlier studies, it is expected that the total carbon content will be reduced to close to the detection limit given enough time.

These results show that electrochemical oxidation can remove the complexing component of s-BTP and PTD by both DEO and with addition of silver (MEO). So, if the presence of these ligands interferes with the oxalate precipitation process DEO could be applied. It is known that the presence of s-BTP and PTD supress the extraction of americium, so during the recycle of the oxalate mother liquor but after evaporation to destroy the oxalic acid, electrochemical oxidation could be applied (with or without silver).

This project has received funding from the EURATOM research and training programme 2014-2018 under grant agreement No 755171. The content of this deliverable reflects only the author's view. The European Commission is not responsible for any use that may be made of the information it contains.

DISCUSION

CONCEPT FLOWSHEET - AHA

AHA is readily decomposed upon evaporation to acetic acid and hydroxylamine [31] and hydroxylamine is rapidly oxidised to gaseous reaction products under the same conditions. The feed to the oxalate precipitation process will contain acetic acid as the main contaminate. To underpin a concept flowsheet for the finishing of actinide products containing AHA the impact of this complexant on oxalate solubility needed to be considered. Although the impact of acetic acid, as a weak complexant, was considered to have an unlikely effect upon actinide oxalate solubility this work has confirmed that earlier hypothesis was correct and that no discernible impact upon solubility occurs. Work under SASCESS showed that acetic acid shows very slow oxidation rate by hot concentrated nitric acid and direct electrochemical oxidation. Mediated electrochemical oxidation gives faster oxidation rates. Consideration of acetic acid – nitric acid vapor liquor evaporation (VLE) establishes that mixed acetic - nitric acid will evaporate together, so under evaporation a proportion of the acetic acid will be distilled to the condensate. It is known that acetic acid has limited impact upon the solvent extraction distribution coefficients. These findings validate that actinide products containing AHA can be processed under the proposed concept flowsheet under consideration, which is the standard industrial oxalate precipitation process adapted for co-precipitation of mixed actinides.

Assuming evaporation is carried to decompose oxalate after oxalate precipitation, further work remains to understand the impact upon:

- Dynamic flowsheet modelling to determine process steady state acetic acid concentrations, which can be used for further assessments,
- Acetic acid in evaporators and condensates from a material compatibility perspective. Likely to be manageable in future reprocessing plants through design,
- Assessment of any additional controls that are necessary to manage the chemical hazards of acetic acid from a chemical safety (flammability) perspective,
- Impacts upon high level waste processing.

However, these remaining wider flowsheet questions are likely to be tolerable or managed through small process changes.

This project has received funding from the EURATOM research and training programme 2014-2018 under grant agreement No 755171. The content of this deliverable reflects only the author's view. The European Commission is not responsible for any use that may be made of the information it contains.

CONCEPT FLOWSHEET: S-BTP

s-BTP is a strong complexant, so it is known that s-BTP must be removed prior to recovery of the actinides from the concentrated oxalate mother liquor (CML). Work has not been conducted to investigate the impact of s-BTP upon oxalate solubility. However, studies have shown that moderately concentrated hot nitric acid and electrochemical oxidation can be used to remove the ability of the solutions to complex with iron(II), based on a colorimetric method. Assuming iron(II) complexing is representative of actinide behaviour, these results suggest that s-BTP can be tolerated in the co-finishing of mixed actinide product.

- If s-BTP affects actinide solubility then, the direct electrochemical oxidation (DEO) can be used.
- If s-BTP does not affect actinide solubility then the effect of hot nitric acid, or direct/mediated electrochemical (DEO or silver MEO) can be applied. Evaporation is currently used in the industrial process, which currently appears adequate.

These results are tentative as the results are at low s-BTP concentrations therefore solvent extraction tests demonstrating the removal of s-BTP complexing effects would be the next logical step in this series of work. Further efforts to monitor decomposition through residual carbon in solution are also needed.

This project has received funding from the EURATOM research and training programme 2014-2018 under grant agreement No 755171. The content of this deliverable reflects only the author's view. The European Commission is not responsible for any use that may be made of the information it contains.

CONCEPT FLOWSHEET - PTD

PTD is a relatively new selective complexing and stripping agent under consideration for current i-SANEX and GANEX-2 flowsheets. This ligand has a relatively complicated structure. As such, it is likely to require a greater degree of consideration compared to AHA, which is a smaller molecule and has simple oxidation products. PTD has limited published work other than distribution coefficients. The key initial finding of this work is that PTD has limited effect upon oxalate solubility, which is further supported by the preparation of mixed oxide in the presence of PTD under GENIORS deliverable 7.4.

As it is known that PTD will increase the routing of minor actinides to the HA raffinate if the PTD is recycled to a solvent extraction process, the remaining key question is how can PTD be removed to prevent this occurring. This work provides an initial assessment of two techniques that could be used, heating in nitric acid (currently used industrially for oxalic acid by evaporation) and electrochemical oxidation. These experiments were carried out at low PTD concentrations due to the limited availability of PTD and as such provide an initial validation of concept. Future work will be needed at actual flowsheet concentrations.

Reflux of PTD in high concentrations of nitric acid show a reduction in the complexant concentration based on an iron(II) colorimetric method. Assuming iron(II) complexation is a good indicator for minor actinide complexation in nitric acid, then these results suggested that heating in hot nitric acid is a good candidate technique prior to feed to solvent extraction. The results in this work suggest that heating of PTD in lower concentrations of nitric acid appears to show an increase in complexing ability of PTD towards iron(II). This is an unexpected result and further work is needed, but it could be rationalised by nitration of PTD. These tests results are relevant to actinide product concentration by evaporation prior to oxalate precipitation. Work is planned to repeat this work at higher PTD concentrations to attempt to replicate these observations. If these findings are repeated, then repeat of solubility studies maybe warranted.

Two electrochemical oxidation tests have been carried out in a small volume equipment using a rotating Nb/BDD electrode. These tests provide an initial comparison of DEO and silver MEO oxidation. These tests suggest the complexing component of PTD, based on iron(II) colorimetric results, reduce quickly by silver MEO and more slowly by DEO. Both techniques show the complexing ability of the solution can be removed within the limit of detection within 6 hours experiment. The total carbon results for DEO and silver MEO do not show a marked reduction and could be explained by the carbon contamination issues in this work but may also suggest a higher stability of the PTD oxidation product, which warrants further investigation. Assuming that the iron(II) complexing results are representative of

This project has received funding from the EURATOM research and training programme 2014-2018 under grant agreement No 755171. The content of this deliverable reflects only the author's view. The European Commission is not responsible for any use that may be made of the information it contains.

minor actinide complexation then, these results suggest that both DEO and silver MEO can be consider as candidate methods for removing the complexing component prior to actinide recovery by solvent extraction. The effect of the non-complexing component of PTD upon solvent extraction chemistry is currently not known.

Based on the results contained within this work and results currently available from GENIORS deliverable 7.4, there appears to be little effect upon the solubility and the chemical form , so the concentrated actinide product containing PTD can be evaporated and conditioned and oxalate precipitated. There remains some uncertainties here as initial tests with PTD in hot nitric acid show an increase in the complexing effectiveness of iron(II) and conditioning with PTD has not been carried out to date. Experiments have shown that the effect of hot nitric acid or electrochemical oxidation, from the limited work, are viable options to remove PTD complexing nature. As hot nitric acid is the most straight forward of these options, as it is already employed to remove oxalic acid prior to recovery of the actinides using the solvent extraction process, this is the preferred option. These results are summarised in the concept flowsheet shown in Figure 46. These results are tentative as the results are at low PTD concentrations and solvent extraction tests demonstrating the removal of PTD complexing effects needs to be considered in a future phase of work.

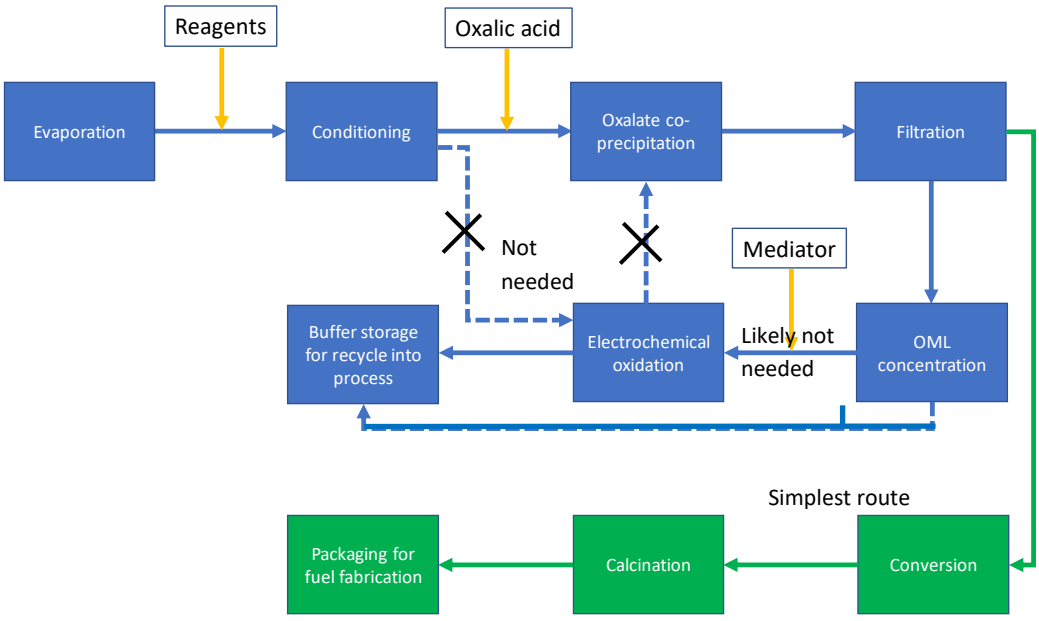

Figure 46: Concept flowsheet for finishing of actinide product containing PTD using oxalate co-precipitation route.

This project has received funding from the EURATOM research and training programme 2014-2018 under grant agreement No 755171. The content of this deliverable reflects only the author's view. The European Commission is not responsible for any use that may be made of the information it contains.

CONCLUSIONS

Actinide solubility – from the work to date, PTD and acetohydroxamic acid and their associated decomposition product (acetic acid) do not affect the solubility of metal ions during oxalate precipitation.

The effect of hot nitric acid under reflux, simulating evaporators, can be used to remove the complexing nature of s-BTP and PTD.

Direct and silver mediated electrochemical oxidation (DEO and MEO(Ag)) can be used to remove the complexing nature of s-BTP and PTD.

These results support the concept flowsheet for the co finishing of actinides via the oxalate route. There are several options; however, the results to date support the simplest concept flowsheet, similar to the current industrial Pu oxalate finishing process, where evaporation is used to destroy oxalic acid and remove the complexing component of PTD. Further studies are needed at represented PTD concentrations to confirm these initial conclusions.

This project has received funding from the EURATOM research and training programme 2014-2018 under grant agreement No 755171. The content of this deliverable reflects only the author's view. The European Commission is not responsible for any use that may be made of the information it contains.

BIBLIOGRAPHY

[1] R. Taylor, Reprocessing and Recycling of Spent Nuclear Fuel, Woodhead Publishing Series in Energy, 2015.

[2] H. Colledge, "A review of alternative finishing options for uranium/plutonium and minor actinide products from thermal and fast reactor fuels reprocessing NNL 15503," National Nuclear Laboratory, Seascale, 2020.

[3] J. P. Patterson and P. Parkes, "Recycling uranium and plutonium," in *The Nuclear Fuel Cycle*, P. Wilson, Ed., Oxford, Oxford University Press, 1996, p. 138.

[4] M. J. Sarsfield, "13 - The coprecipitation and conversions of mixed actinide oxalates for aqueous-based reprocessing of spent nuclear fuels," in *Reprocessing and recycling of spent nuclear fuel*, Seascale, Woodhead Publishing, 2015, pp. 325-351.

[5] P. Wilison, The nuclear fuel cycle: from ores to wastes, Oxford Science Publications, 1997.

[6] CEA, Treatment and recycle of spent fuel, CEA, DEN monographs, 2008.

[7] F. Abraham, B. Arab-Chapelet, M. Rivenet, C. Tamain and S. Grandjean, "Actinide oxalates, solid structures and applications," *Coordination Chemistry Reviews,* Vols. 266-267, pp. 28-68, 2014.

[8] E. D. Collins, "12 - Advanced thermal denitration conversion processes for aqueous-based reprocessing and recycling of spent nuclear fuels," in *Reprocessing and Recycling of Spent Nuclear Fuel*, Oak Ridge, Woodhead Publishing, 2015, pp. 313-323.

[9] M. A. Pouchon, "14 - Gelation and other innovative conversion processes for aqueous-based reprocessing and recycling of spent nuclear fuels," in *Reprocessing and Recycling of Spent Nuclear Fuel*, Villigen, Woodhead Publishing , 2015, pp. 353-369.

This project has received funding from the EURATOM research and training programme 2014-2018 under grant agreement No 755171. The content of this deliverable reflects only the author's view. The European Commission is not responsible for any use that may be made of the information it contains.

[10] J. M. Cleveland, “Chapter 15: Plutonium conversion process,” in *PLutonium Handbook. A guide to the technology - Volume I & II*, O. J. Wick, Ed., La Grange Park, American Nuclear Society, 1980, pp. 553-572.

[11] C. Mason, T. Brown, D. Buchanan, C. Maher, D. Morris and R. Taylor, “The Decomposition of Oxalic Acid in Nitric Acid,” *Journal of Solution Chemistry*, vol. 45, pp. 325-333, Feb 2016.

[12] D. Yong Chung and E. Hee Lee, “Kinetics of the Hydrolysis of Acetohydroxamic Acid in a Nitric,” *J. Ind. Eng. Chem,* pp. 962-966, 2006.

[13] M. R. Bennett, L. Maya, G. M. Brown and F. A. Posey, “Oxidation of hydroxylamine by nitrous and nitric acids,” *Inorganic Chemistry,* p. 2461–2468, 1982.

[14] S. Reilly, C. Maher, S. Brewer and R. Taylor, “Decomposition studies of aqueous phase ligands used in advanced,” *Procedia Chemistry,* vol. 21, pp. 530-535, 2016.

[15] J. H. Miles, “Separation of plutonium and uranium,” *Science and technology of tributyl phosphate,* vol. 111, pp. 11-54, 1990.

[16] R. Taylor and G. Mathers, “Innovation in the aqueous recycle of spent nuclear fuels,” *Nuclear Future,* vol. 15, pp. 40-48, 2019.

[17] W. B. Kerr, “Production test 234-5 plant process evaluation precipitation of plutonium IV oxalate HW-26450,” Hanford Works, Richland, 1952.

[18] J. M. Cleveland, The Chemistry of Plutonium, La Grange Park : American Nuclear Society, 1979.

[19] S. Grandjean, B. Arab-Chapelet, A. C. Robisson, F. Abraham, P. Martin, J. P. Dancausse, N. Herlet and C. Leorier, “Structure of mixed U(IV)-An(III) precursors synthesized by co-conversion methods (where An = Pu, Am or Cm),” *Journal of Nuclear Materials,* vol. 385, no. 1, pp. 204-207, 2009.

This project has received funding from the EURATOM research and training programme 2014-2018 under grant agreement No 755171. The content of this deliverable reflects only the author’s view. The European Commission is not responsible for any use that may be made of the information it contains.

[20] B. Arab-Chapelet, S. Grandjean, G. Nowogrocki and F. Abraham, “Synthesis and characterization of mixed An(IV)An(III) oxalates (An (IV) = Th, Np, U or Pu and An(III) = Pu or Am),” *Journal of Nuclear Materials,* vol. 373, no. 1-3, pp. 259-268, 2008.

[21] T. S. Rubisill, “Solubility of Plutonium (IV) Oxalate During Americium/Curium PretreatmentWSRC-TR-99-00162,” Westinghouse Savannah River Company, Aiken, 1999.

[22] C. H. Delegard, S. I. Sinkov, B. K. McNamara, S. A. Jones, G. S. Barney , A. J. Schmidt and R. L. Sell, “Critical mass laboratory solutions precipitation,calcination and moisture uptake investigations PNNL-13934,” Pacific Northwest National Laboratory, 2002.

[23] D. T. Rankin, W. R. Kanne, D. F. Bickford, M. R. Louthan and J. W. Congdon, “Production of Pu-238 oxide fuel for space exploration,” in *50 years of excellence in science and engineering at the Savannah River Site*, Aiken, 2000.

[24] G. A. Burney and P. K. Smith, “Controlled PuO2 Particle Size From Pu(III) Oxalate Precipitation,” E.I. du Pont de Nemours & Co, Aiken, 1984.

[25] R. M. Greintz and D. H. Neal, “Plutonium(III) oxalate precipitation and calcination process for plutonium nitrate to oxide conversion RFP-2603,” Rockwell International Energy Systems Group, Golden, 1980.

[26] R. S. Herbst, P. Baron and M. Nilsson, “6 - Standard and advanced separation: PUREX processes for nuclear fuel reprocessing,” in *Advanced Separation Techniques for Nuclear Fuel Reprocessing and Radioactive Waste Treatment*, K. L. Nash and G. J. Lumetta, Eds., Woodhead Publishing, 2011, pp. 141-175.

[27] G. Modolo, A. Geist and M. Miguirditchian, “10 - Minor actinide separations in the reprocessing of spent nucelar fuels:recent advances in Europe,” in *Reprocessing and Recycling of Spent Nuclear Fuel*, R. Taylor , Ed., Woodhead Publishing, 2015, pp. 245-287.

This project has received funding from the EURATOM research and training programme 2014-2018 under grant agreement No 755171. The content of this deliverable reflects only the author’s view. The European Commission is not responsible for any use that may be made of the information it contains.

[28] G. Modolo, A. Wilden, P. Kaufholz, D. Bosbach and A. Geist, "Development and demonstration of innovative partitioning processes (i-SANEX and 1-cycle SANEX) for actinide partitioning," *Progress in Nuclear,* vol. 72, pp. 107-114, 2014.

[29] M. Miguirditchian, V. Vanel, C. Marie, V. Pacary, M. Charbonnel, L. Berthon, X. Heres, M. Montuir, C. Sorel, M. Bollesteros, S. Costenoble, C. Rostaing, M. Masson and C. Poinssot, "Americium recovery from highly active: PUREX raffinateby solvent extraction: the EXAm process. A review of 10 years of R&D," *Solvent Extraction and Ion Exchange,* vol. 38, no. 4, pp. 365-387, 2020.

[30] E. J. Birkett, M. J. Carrott, D. O. Fox, C. J. Jones, C. J. Maher, C. V. Roube, R. J. Taylor and D. A. Woodhead, "Developments in the PUREX process for nuclear fuel reprocessing: Complexant based stripping for uranium/plutonium separation," *CHIMIA International Journal for Chemistry,* vol. 59, pp. 898-904, 2005.

[31] M. J. Carrott, D. O. Fox, G. LeGurun, C. J. Jones, C. Mason, R. Taylor, F. Andrieux and C. Boxall, "Oxidation-reduction reactions of simple hydroxamic acids and plutonium(IV) ions in nitric acid," *Radiochimica Acta,* vol. 96, no. 6, pp. 333-344, 2008.

[32] E. Mossini, E. Macerata, A. Wilden, P. Kaufholz, G. Modolo, N. Lotti, A. Casnati, A. Geist and M. Mariani, "Optimization and single-stage centrifugal contactor experiments with the novel hydrophillic complexant PyTri-Diol for the i-SANEX process," *Solvent Extraction and Ion Exchange,* vol. 36, no. 4, pp. 373-386, 2018.

[33] G. A. Burney and J. A. Porter, "Solubilities of Pu(III), Am(III), and Cm(III) oxalates," *Inorganic and Nuclear Chemistry Letters,* vol. 3, no. 3, pp. 79-85, 1967.

[34] S. P. Hasilkar, N. B. Khedekar, K. Chander, A. V. Jadhav and H. C. Jain, "Studies on the solubility of Pu(III) oxalate," *Journal of Radioanalytical and Nuclear Chemistry,* vol. 185, pp. 119-125, 1994.

[35] M. Borkowski, R. C. Moore, M. G. Bronikowski, J. Chen, O. S. Pokrovsky, Y. Xia and G. R. Choppin, "Thermodynamic modeling of actinide complexation with oxalate at high

This project has received funding from the EURATOM research and training programme 2014-2018 under grant agreement No 755171. The content of this deliverable reflects only the author's view. The European Commission is not responsible for any use that may be made of the information it contains.

ionic strength," *Journal of Radioanalytical and Nuclear Chemistry,* vol. 248, pp. 467-471, 2001.

[36] D. Ferri, M. Iuliano, C. Manfredi, E. Vasca, T. Caruso, M. Clemente and C. Fontanella, "Dioxouranium(VI) oxalate complexes," *Journal of the Chemical Society, Dalton Transactions,* vol. 19, pp. 3460-3466, 2000.

[37] P. Thakur, J. N. Mathur, R. C. Moore and G. R. Choppin, "Thermodynamics and dissociation constants of carboxylic acids at high ionic strength and temperature," vol. 360, no. 12, pp. 3671-3680, 2007.

[38] W. Hummel, G. Anderegg, I. Puigdomenech, L. Rao and O. Tochiyama, "Chemical thermodynamics of compounds and complexes of U, Np, Pu, Am, Tc, Se, Ni and ZR with selected organics ligands," *Chemical Thermodynamics,* vol. 9, p. 1130, 2005.

[39] C. J. Mandleberg, K. E. Francis and R. Smith, "The solubility of plutonium trifluoride, plutonium tetrafluoride, and plutonium(IV) oxalate in nitric acid mixtures," *Journal of the Chemical Society,* p. 2464, 1961.

[40] P. R. O'Connor, "Metallurgical Laboratory Report CN-1702," Univeristy of Chicago, 1944.

[41] A. I. Moskvin and A. D. Gel'man, "Determination of composition and instability constants of oxalate and carbonate complexes of plutonium," *Soviet Journal of Inorganic Chemistry,* vol. 3, pp. 962-974, 1958.

[42] P. Richard, "Procédé continu de précipitation des sels de plutonium CEA-R3198," Commisariat à l'Energie Atomique , 1967.

[43] J. M. Berg, D. K. Veirs, R. B. Vaughn, M. A. Cisneros and C. A. Smith, "PLutonium(IV) mononitrate and dinitrate complex formation in acidsolutions as a function of ionic strength," *Journal of Radioanalytical and Nuclear Chemistry,* vol. 235, pp. 25-29, 1998.

This project has received funding from the EURATOM research and training programme 2014-2018 under grant agreement No 755171. The content of this deliverable reflects only the author's view. The European Commission is not responsible for any use that may be made of the information it contains.

[44] P. R. Monson Jr. and R. Hall, “Thorium oxalate solubility and morphology,” Du Pont de Nemours (E.I) and Co, Aiken, 1981.

[45] J. A. Porter and A. E. Symonds Jr., “Precipitation of plutonium(III) oxalate and calcination to plutonium dioxde DP-981,” E. I. du Pont de Nemours & Co Savannah River Laboratory, Aiken, 1965.

[46] S. L. Yarbro, S. B. Schreiber, S. L. Dunn and C. W. Mills, “Automated homogeneous oxalate precipitation of Pu(III),” Los Alamos National Lab (LANL), Los Alamos, 1990.

[47] K. M. Harmon and W. H. Reas, “Conversion chemistry of plutonium nitrate HW-49597,” Hanford Atomics Products Operation, Richland, 1957.

[48] J. S. Griffo, W. B. Brown and F. D. Lonadier, “Solubility of plutonium compounds MLM-1191,” Mound Lab, Miamisburg, 1963.

[49] S. L. Yarbro, S. B. Schreiber, S. L. Dunn and C. W. Mills, “Homogeneous oxalate precipitationof Pu(III),” in *Transuranium Elements Symposium*, 1992.

[50] R. J. Lemiere, J. Fuger, H. Nitsche, P. Potter, M. H. Rand, J. Rydberg, K. Spahiu, J. C. Sullivan, W. J. Ullman, P. Vitorgg and H. Wanner, “Chemical Thermodynamics of Neptunium and Plutonium,” in *Chemical Thermodynamics Volume 4*, Issy-les Moulineaux, Nuclear Energy Agency, 2001, p. 870.

[51] T. Fanghanel, J. Fuger, I. Grenthe, V. Neck, D. A. Palmer and M. H. Rand, Update on the chemical thermodynamics of uranium, neptunium, plutonium, americium and technetium, Issy-les-Moulineaux: Chemical Thermodynamics Volume 5, 2003.

[52] O. Tuck, “Experimental design for Pu solubility experiments,” BEIS10998/06/10/04 - Issue 1, 2020.

[53] G. L. S. A. A. Traister, “Water-Soluble Sulfonated Chromogenic Reagents of the Ferroin TYpe and Determination of Iron and Copper in Water, Blood, Serum, and Beer with the

This project has received funding from the EURATOM research and training programme 2014-2018 under grant agreement No 755171. The content of this deliverable reflects only the author’s view. The European Commission is not responsible for any use that may be made of the information it contains.

Tetraammonium Salt fo 2,4-Bis(5,6-diphenyl-1,2,4-triazin-3-yl)pyridinetetrasulfonic Acid," *Analytical Chemistry,* vol. 48, no. 8, pp. 1216 - 1220, 1976.

[54] I. Herdzik-Koniecko, C. Wagner, M. Trumm, U. Müllich, B. Schimmelpfennig, J. Narbutt, A. Geist and P. Panak, "Do An(iii) and Ln(iii) ions form heteroleptic complexes with diglycolamide and hydrophilic BT(B)P ligands in solvent extraction systems? A spectroscopic and DFT study," *New Journal of Chemistry,* vol. 43, pp. 6314-6322, 2019.

[55] G. Taylor, "Development of electrochemical oxidation using boron doped diamond-coated film electrodes for the the treatment of waste lubricants: Part 1 assessment of potential," in *WM '05* , Tuscan, AZ, 2005.

This project has received funding from the EURATOM research and training programme 2014-2018 under grant agreement No 755171. The content of this deliverable reflects only the author's view. The European Commission is not responsible for any use that may be made of the information it contains.